NASA TECHNICAL MEMORANDUM

NASA TM X-3448

NASA TM X-3448

DESCRIPTION AND OPERATING PERFORMANCE OF A PARALLEL-RAIL ELECTRIC-ARC SYSTEM WITH HELIUM DRIVER GAS FOR THE LANGLEY 6-INCH EXPANSION TUBE

John A. Moore

Langley Research Center

Hampton, Va. 23665

NATIONAL AERONAUTICS AND SPACE ADMINISTRATION • WASHINGTON, D. C. • DECEMBER 1976

1. Report No.	2. Government Accession No.	3. Recipient's Catalog No.
NASA TM X-3448		

4. Title and Subtitle	5. Report Date
DESCRIPTION AND OPERATING PERFORMANCE OF A PARALLEL-RAIL ELECTRIC-ARC SYSTEM WITH HELIUM DRIVER GAS FOR THE LANGLEY 6-INCH EXPANSION TUBE	December 1976
	6. Performing Organization Code
7. Author(s)	8. Performing Organization Report No.
John A. Moore	L-11109
	10. Work Unit No. 506-26-20-01
9. Performing Organization Name and Address NASA Langley Research Center Hampton, VA 23665	11. Contract or Grant No.
	13. Type of Report and Period Covered Technical Memorandum
12. Sponsoring Agency Name and Address National Aeronautics and Space Administration Washington, DC 20546	14. Sponsoring Agency Code

15. Supplementary Notes

16. Abstract

A description of a parallel-rail arc-discharge system to heat and pressurize the initial helium driver gas of the Langley 6-inch expansion tube is presented. This system was designed for a 2.44-m-long driver vessel rated at 138 MPa, with a distance between rails of 20.3 cm. Electric energy was obtained from a capacitor storage system rated at 12 000 V with a maximum energy of 5 MJ. Tests were performed over a range of energy from 1.74 MJ to the maximum value. The operating experience and system performance are discussed, along with results from a limited number of expansion-tube tests with air and carbon dioxide as test gases.

17. Key Words (Suggested by Author(s))	18. Distribution Statement
Arc discharge Impulse facility Expansion tube Shock tube	Unclassified - Unlimited Subject Category 09

19. Security Classif. (of this report)	20. Security Classif. (of this page)	21. No. of Pages	22. Price*
Unclassified	Unclassified	38	$3.75

* For sale by the National Technical Information Service, Springfield, Virginia 22161

DESCRIPTION AND OPERATING PERFORMANCE OF A PARALLEL-RAIL ELECTRIC-ARC SYSTEM WITH HELIUM DRIVER GAS FOR THE LANGLEY 6-INCH EXPANSION TUBE

John A. Moore
Langley Research Center

SUMMARY

A description of a parallel-rail arc-discharge system to heat and pressurize the initial helium driver gas of the Langley 6-inch expansion tube is presented. This system was designed for a 2.44-m-long driver vessel rated at 138 MPa, with a distance between rails of 20.3 cm. Electric energy was obtained from a capacitor storage system rated at 12 000 V with a maximum energy of 5 MJ. Tests were performed over a range of energy from 1.74 MJ to the maximum value. The operating experience and system performance are discussed, along with results from a limited number of expansion-tube tests with air and carbon dioxide as test gases.

For the range of electrical energy investigated, the efficiency of conversion from electrical to thermal energy, as inferred from the measured incident shock velocity in the test gas, varied from approximately 30 to 85 percent. Visual inspection of the rails immediately following a test indicated that the arc traveled a distance of approximately 1 m along the 1.93-m-long rail at the maximum energy level of 5 MJ. Measured time histories of the pressure in the driver vessel revealed the existence of a series of strong shocks generated in the helium driver as the result of the arc discharge; this nonuniformity in driver-gas pressure with time resulted in a degradation in the wall-pressure time histories in the driven section. A number of problems with the hardware were encountered, resulting in a long turnaround time for the parallel-rail system; solutions to many of the problems are discussed. Because of the long turnaround time, only a limited number of tests were performed to evaluate expansion-tube performance. These tests revealed that the arc-drive mode increased facility performance in terms of generation of higher velocities, but test-section flow quality, for the conditions of this study, was poor.

INTRODUCTION

As discussed in reference 1, idealized performance predictions for the expansion tube (ref. 2) and the expansion tunnel (ref. 3) indicated that free-stream density and velocity could be varied over wide ranges. This versatility in performance could, theoretically, be achieved by proper selection of parameters such as the driver mode, the initial pressures in the various chambers, and the proportionate chamber lengths. Thus the facility consisting of the Langley 6-inch expansion tube and the Langley expansion tunnel was designed for a number of different modes of operation. Its development has consisted, in

part, of the study of several of these combinations of options in order to compare the actual performance of the expansion tube with its predicted performance.

In an expansion tunnel the test gas undergoes two expansion processes. The first is an unsteady expansion (ref. 2) which produces the flow state at the expansion-tube exit or expansion-tunnel nozzle entrance; the second is a steady expansion as the flow traverses the nozzle. For this second expansion, the velocity change between the nozzle entrance and nozzle exit is relatively small (ref. 4), whereas the density change in the nozzle expansion is dependent on the nozzle area ratio and may decrease significantly. If the density of the nozzle entrance flow is too small, the corresponding lower density at the nozzle exit may produce undesirable effects such as loss of schlieren sensitivity, long chemical relaxation rates, or noncontinuum flow. Thus, in the case of the expansion tunnel, it is desirable to supply a high-density, quasi-steady flow at the nozzle entrance.

To obtain the higher densities required for successful expansion-tunnel operation, higher densities must be generated in the region behind the incident shock into the quiescent test gas. It is well recognized that the same shock velocity may be obtained at higher test-gas density levels if the pressure and speed of sound of the driver gas are increased. This is commonly achieved by a rapid discharge of electrical energy, stored in a high-voltage capacitor system, into a quiescent driver gas. For shock tubes, the driver sections are, in general, relatively short, and a coaxial electrode arrangement is used in which the arc is drawn from an upstream anode along the axis to an electrode in the vicinity of the diaphragm. However, for the expansion tunnel, much longer driver lengths are required for the high-density operating range. This is due to the slower incident shock velocities into the relatively high-pressure quiescent test gas required for the high-density operation of the expansion tunnel, as compared with an arc-driven shock tube. For these lower incident shock velocities, the expansion wave reflected from the end of a short driver tends to catch up with the test gas. As reported in reference 5, arc lengths up to 2.54 m have been drawn with a coaxial electrode arrangement. This was achieved by using a 40-kV capacitor system. For the Langley expansion tunnel the available capacitor system is rated at 12 kV, which is not sufficient to draw an arc the length of the 2.44-m-long driver section with a coaxial electrode arrangement such as that tested in reference 5.

To approximate a uniform temperature distribution along the expansion-tunnel driver section, a parallel-rail electrode arrangement was designed and fabricated for the Langley 6-inch expansion tube (ref. 6). Two parallel electrodes, or rails, extend from the upstream end of the driver section to near the diaphragm at the downstream end of the driver. These electrodes are connected, through coaxial electrical leads, to the capacitor energy storage system. Upon initiation of the arc discharge across these rails, the arc moves from the upstream end of the rails and along the rails toward the diaphragm by means of self-induced electromagnetic forces.

The performance of this parallel-rail electrode arrangement as a method for heating the helium driver gas in the Langley 6-inch expansion tube is the subject of this paper. Current and voltage measurements were made for a range

of initial stored energy levels, and the resulting pressure time histories of the helium driver gas were measured. The efficiency of conversion from electrical to thermal energy was inferred from the measured incident shock velocity into the quiescent air or carbon dioxide test gas. A limited number of runs were performed with instrumentation located at the test section of the expansion tube in an effort to determine test time, flow uniformity, and flow conditions.

SYMBOLS

$\vec{B}$	magnetic induction vector
b	damping exponent, R/2L
C	capacitance, F
E	energy, J
I	current, A
$\vec{J}$	current density vector
L	inductance, H
p	pressure, Pa
p_t	pitot pressure, Pa
Q	charge, C
R	resistance, Ω
R_{cr}	resistance for critical damping, Ω
T	temperature, K
t	time, s
U_s	incident shock velocity, m/s
V	potential difference, V
v	volume, m^3
x	axial distance downstream of primary diaphragm, m
γ	ratio of specific heats
δ	phase angle, arc tan (ω'/b)

η efficiency (see eq. (1))

ω $= 1/\sqrt{LC}$, rad/s

ω' $= \sqrt{\omega^2 - b^2}$, rad/s

Subscripts:

d driver

i initial conditions in driver vessel

max maximum

1 initial state in intermediate or driven section

4 driver-gas conditions at time of primary diaphragm rupture

10 initial state in acceleration section

DESCRIPTION OF SYSTEM

A sketch of the Langley 6-inch expansion tube is presented in figure 1, and a description and initial operating performance of the facility and its associated equipment are given in reference 6.

The parallel-rail electric-arc assembly was designed for the 2.44-m-long, 35.6-cm inside diameter, driver vessel shown in figure 2. The driver vessel was fabricated from ASTM A336 Type F8-304 stainless steel (nonmagnetic), and designed to withstand a maximum pressure of 138 Pa. Photographs of various components of the electric-arc drive assembly are shown in figure 3. The insulators are made of fiberglass and epoxy resin, except for the fluorogreen insulator at the upstream end of the assembly just behind the trigger-wire connection. The parallel rails were fabricated from beryllium copper, are 2.08 m long, and extend from the coaxial feed to within 21 cm of the steel diaphragm at the downstream end of the driver vessel. The rails are bolted to the main insulator, which has a 35.6-cm outside diameter and a 27.6-cm inside diameter, both to support the weight of the rails and to withstand the possible loading from the pressure differentials across the rails. The rails are spaced 20.3 cm apart and each rail is 4 cm from the driver vessel wall. A trigger wire was anchored in the ground potential rail about 30 cm from the upstream end of the assembly, looped up near the high-potential rail, and then connected to the trigger-wire lead.

Unreported experience with a parallel-rail electric-arc drive assembly in the Langley pilot model expansion tube (see ref. 7 for a description of this facility) indicated that high currents in the rails close to the driver vessel

walls induced eddy currents in the walls. The interaction of the electromagnetic fields produced by these currents and the currents in the rails resulted in forces on the rails large enough to drive them together and cause failure at the juncture of the rails and the coaxial feed. Based on this experience, the spacing of the rails and the distance from the rails to the wall were chosen to balance the forces due to the current in the two rails and the eddy currents in the vessel walls.

A schematic of the electrical circuit is shown in figure 4. The energy to drive the electric-arc discharge is stored in a 10-MJ capacitive energy storage system that is shared with the arc-driven Langley 6-inch shock tube (ref. 8). This system consists of four banks of capacitors and a charging unit. Each bank of capacitors is made up of approximately 800 individual capacitors (fig. 3(g)), and these individual capacitors are rated at 12 000 V and 43 μF of capacitance. Groups of 10 capacitors are connected by means of a coaxial cable to a coaxial collector assembly (fig. 3(f)). One collector serves each bank of 800 capacitors. This permits the banks to be used separately or in parallel. A coaxial feed (fig. 3(e)) leads from the collector to the parallel-rail assembly in the driver vessel. The energy storage capacitors are charged through the collector assembly by means of cables leading to the charging unit.

The energy for the trigger wire is stored in one group of 10 capacitors that are charged concurrently with the main bank of capacitors. A switch is used to connect the bank of 10 capacitors to the coaxial cable leading to the trigger wire to initiate the discharge.

THEORY OF OPERATION

The operation of the parallel-rail electric arc is based on the well-known law of interaction of electromagnetic fields produced by adjacent current-carrying conductors. The driver vessel is evacuated and then filled with helium. (In the present study, the quiescent helium driver-gas pressure was 2.07 Pa.) The trigger wire is energized and evaporated, forming a low-resistance path between the two rails. Current moves down one rail, along this low-resistance path, and back along the other rail. The heated column of helium plasma acts as a current-carrying conductor, resulting in an interaction with the electromagnetic fields produced by the currents in the rails. The force on this plasma column, or arc, is due to the vector product $\vec{J} \times \vec{B}$ (denoted as the law of Biot and Savart in ref. 9), where $\vec{J}$ is the current density vector in the circuit and $\vec{B}$ is the magnetic field vector generated by the presence of current in the rails. The force on the helium gas plasma conducting the current between the rails moves the plasma at a right angle to both the direction of current flow in the plasma and the direction of the magnetic field produced by the current in the rails. The direction of this force is parallel to the length of the rails and oriented toward the portion of the rails in which the current is not flowing. The plasma column of helium gas moves down the length of the rail under the influence of the $\vec{J} \times \vec{B}$ force and the fluid dynamic drag.

INSTRUMENTATION

Current and Voltage

The voltage and current for the electric-arc drive were measured at the coaxial collector assembly, as indicated in the schematic of figure 4. A 50-cm-diameter Rogowski (toroidally wound) coil was placed around the inner conductor of the coaxial feed to measure the current (fig. 3(e)). The output of the coil is a measure of the rate of change of the current, and the integration of this output using an operational amplifier yields the current as a function of time. High-voltage attenuator probes were used to measure the voltage on the center high-potential lead, the voltage on the outer ground-potential lead, and the voltage on the trigger-wire lead. The attenuated trigger voltage was used to trigger the oscilloscopes on which voltage, current, accelerometer, and the output signals of the driver pressure transducer were recorded.

Pressure

The wall-pressure time history in the driver vessel, driven section and acceleration section, and the pitot-pressure time histories at the exit of the acceleration section were measured with piezoelectric (quartz) transducers. The output signals were processed by charge amplifiers and recorded on oscilloscopes. Since piezoelectric transducers are sensitive to temperature, a coating of silicone room-temperature-vulcanizing rubber was applied to the sensing surface of all pressure transducers for thermal protection. Calibration of the transducers showed no effect of the coating on the transducer output for a given pressure applied to the sensing surface. Pitot-pressure transducers were protected from particle damage by an overlapping baffle arrangement, as described in reference 6.

Velocity

One method used to infer the incident shock velocity in the driven section and the acceleration section was the microwave interferometer system (ref. 10). The application of this system to the present facility is described in reference 6. Because of insufficient electron density at the shock front, the microwave system did not track the incident shock in the driven section when either carbon dioxide (CO_2) was used as a test gas, or air at the highest initial pressure was used as the test gas. For these conditions, the time-of-arrival method (ref. 11) was used; that is, the time of shock arrival at measured intervals along the length of the tube was detected by pressure transducers and heat transfer gages mounted flush with the wall surface. Velocity was determined from a faired curve through the data plotted as arrival time against distance along the tube. Only approximate values of the incident shock velocity in the driven section could be determined because of the limited number of instrumented stations in this section. Uncertainties in the velocity measurements are discussed in reference 11.

DATA REDUCTION

Efficiency

It is useful to determine the efficiency of the electric arc in transforming the electrical energy stored in the capacitors to internal energy of the driver gas. This efficiency may then be used to help predict facility performance. The efficiency calculation is based on the assumption that the energy transfer is completed before the diaphragm opens (constant volume process) and the heated driver gas is isotropic. (See, for example, ref. 12 for a discussion of the efficiency calculation.) The efficiency is then defined as the change in internal energy of the driver gas divided by the initial energy stored in the capacitors. Using perfect gas relations, the efficiency can be expressed as

$$\eta \equiv \frac{p_4 - p_i}{\gamma_4 - 1} \frac{v}{E} \tag{1}$$

where p_i is the initial driver-gas pressure, p_4 is the driver-gas pressure at the time of the primary diaphragm rupture, v is the net volume of the driver chamber, γ_4 is the ratio of specific heats of the driver gas, and E is the energy stored in the capacitors.

The efficiency can be determined from equation (1) if the pressure p_4 is known, since determination of the other terms on the right side of the equation is straightforward. Measurement of the postdischarge driver pressure is very difficult, as will be shown subsequently, and such measurements may not represent the average pressure in the driver at the time of the diaphragm rupture. The rapid discharge of energy at some point in the driver vessel induces a shock-wave system which is very complex as a result of reflection from the driver walls, and thus a wall-pressure measurement is dominated by the influence of the impinging shock waves.

Because of the difficulties associated with the measurement of p_4, the efficiency is frequently inferred from the velocity of the incident shock wave in the driven gas (e.g., refs. 8 and 12). Figure 5 shows an example of the method used. Real gas effects of the driven gas are considered since the calculations of reference 13 were used for equilibrium air and the calculations of reference 14 were used for carbon dioxide in this method. In figure 5 (which corresponds to fig. 5 of ref. 13), the shock-wave velocity is shown as a function of the diaphragm pressure ratio p_4/p_1 for several values of the driver-gas temperature T_4. Using the initial diaphragm pressure ratio p_i/p_1 and noting that at constant volume $p_4/p_i = T_4/T_i = T_4/T_1$, the dashed curve in figure 5 is constructed. Using the dashed curve and the measured shock-wave velocity, an effective diaphragm pressure ratio, and hence a value of p_4, may be determined. The efficiency may be determined with the use of equation (1).

While the values of p_4 determined by the method just described are somewhat hypothetical, the efficiency computed using this value of p_4 can be mean-

ingful. When the observed shock velocity is used in computing the efficiency, the result includes not only the energy transfer efficiency but also the nonideal effects of the shock formation process. Thus, performance estimates using this efficiency may be expected to give realistic estimates of the shock velocity.

Circuit Constants

The inductance, resistance, voltage, and current of the electrical circuit were determined in the present study, since a knowledge of the values of these parameters can be of help when an effort is made to improve the design and efficiency of the electric-arc-discharge system. As discussed previously, voltage and current were measured as a function of time and typical records of the voltage and current during discharge are shown in figure 6. To obtain approximate values of inductance and resistance several assumptions are made. First, the contribution of the resistance and inductance of the storage capacitors, coaxial cables, and coaxial collectors is assumed to be negligible compared with that of the coaxial feed, parallel rail, and arc during the time of discharge of electrical energy (fig. 4). Second, the inductance L, resistance R, and capacitance C are assumed constant, although it is realized that L and R in an arc may vary with current. With these assumptions, the linear ordinary differential equation for the charge in an electrical circuit, with resistance, capacitance, and inductance in series, is

$$L \frac{d^2Q}{dt^2} + R \frac{dQ}{dt} + \frac{1}{C} Q = 0 \tag{2}$$

The solution for an oscillatory, or underdamped, condition with an initial condition of zero current and charge Q equal to the charge on the storage capacitors is

$$Q = Q_{t=0} e^{-bt} \left[\cos (\omega^2 - b^2)^{1/2} t + \frac{b}{(\omega^2 - b^2)^{1/2}} \sin (\omega^2 - b^2)^{1/2} t \right] \tag{3}$$

which can be reduced to

$$Q = Q_{t=0} \frac{\omega}{\omega'} e^{-bt} \sin (\omega' t + \delta) \tag{4}$$

where

$$b = \frac{R}{2L} \quad , \quad \omega = (LC)^{-1/2} \quad , \quad \omega' = (\omega^2 - b^2)^{1/2} \quad , \quad \delta = \arctan \frac{\omega'}{b} \tag{5}$$

In terms of the voltage across the capacitors, the relation $Q = CV$ yields

$$V = V_{t=0} \frac{\omega}{\omega'} e^{-bt} \sin(\omega' t + \delta) \tag{6}$$

Since the current is the rate of change of the charge, then by differentiation of equation (4) the current is

$$I = Q_{t=0} \frac{\omega^2}{\omega'} e^{-bt} \sin(\omega' t) \tag{7}$$

Measurement of the time at which the current goes to zero gives a value for ω' from equation (7), and this value of ω' and the time at which the voltage goes to zero gives a value for δ from equation (6). For these values of ω' and δ, corresponding values for b and ω, and hence L and R, may be calculated by using relations in equation (5) and the known value of the capacitance C in the energy storage system.

As mentioned previously the voltage and current were measured at the coaxial collector assembly, and thus the calculated inductance and resistance values are the lumped values for the entire circuit. A value for the effective inductance of the circuit preceding the point at which the voltage is measured (fig. 4) can be determined by measuring the initial voltage at the collector and the initial rate of change of current, both measured at the time current begins to flow.

TEST CONDITIONS

The volume of the driver vessel with the parallel-rail assembly installed was 0.0964 m^3. For all tests reported herein, this volume was first evacuated to approximately 15 Pa and then filled with helium to a pressure of 2.07 MPa. The energy level was determined by the charge voltage and the use of either one or two banks of capacitors. The capacitance of each bank of 800 capacitors was 0.0347 F. The maximum energy available in each bank was 2.5 MJ.

As noted in reference 6, a stainless steel diaphragm with a cross-pattern groove separates the driver and intermediate sections. For the present tests, the diaphragm was 5.1 mm thick and the groove was scribed to a depth such that the thickness of metal left was 2.5 mm. The static rupture pressure for this diaphragm was approximately 24 MPa. The facility was operated both as an expansion tube and a shock tube. For the expansion-tube mode of operation, the intermediate section was 4.65 m long and the acceleration section was 16.98 m long. A 6.35-μm-thick mylar diaphragm separated the intermediate and acceleration sections. For shock-tube runs, the mylar diaphragm was removed, providing a driven section length equal to 21.63 m.

The test gas was either air or CO_2. The quiescent or initial pressures for CO_2 were 24.13 and 48.26 kPa, and the initial pressures for air were 6.89 and 48.26 kPa. For expansion-tube tests, the acceleration gas was the same as the test gas, except for one run in which helium was used as the acceleration gas and air as the test gas. Initial conditions for the tests reported herein are given in table 1.

RESULTS AND DISCUSSION

Values of the resistance, inductance, and frequency of the circuit for each run, as determined from the voltage and current time histories, are given in table 2. The inductance of the circuit is approximately 0.55 μH and the resistance ranges from approximately 2 to 4 mΩ. The inductance of the circuit from the energy storage capacitors to the collector was determined to be approximately 0.04 μH. The resistance of this part of the circuit could not be determined from measurements but was calculated to be extremely small, since all cables and capacitors were in parallel.

The measured values of maximum current for various values of initial stored energy are shown in figure 7. These measured values are compared with predicted values of maximum current using equation (7). A nominal value of the inductance, 0.55 μH, was used to predict the current for values of resistance equal to 2, 3, and 4 mΩ for both one and two banks of capacitors (C = 0.0347 and 0.0694 F, respectively). For the range of conditions illustrated in figure 7, the experimental data essentially fall within the region encompassed by the predictions for values of resistance equal to 2 and 3 mΩ for both one and two banks of capacitors. Hence, the simplifying assumptions made to obtain equations (3) to (7) appear to be reasonably good for the present study. This analysis demonstrates that maximum values of current for the present electrical system can be predicted with fair accuracy by using a value of inductance L equal to 0.55 μH and a value of R equal to 2.5 mΩ for values of capacitance ranging from 0.0347 to 0.0694 F and energies from 1.74 to 5.0 MJ.

It should be noted that the resistance values determined in the present experiment were not the net resistance across the arc, since they included the resistance from the points of voltage measurement to the arc location. Since neither the value of the voltage drop across the arc nor the net arc resistance was obtained in the present experiment, it was not possible to determine a measured value of electrical energy expended in the arc.

Measured pressures in the driver vessel are presented in figure 8 as a function of time. A value of time equal to zero corresponds to the initial increase in pressure above the quiescent value, as read from oscilloscope film traces. This initial rise in pressure occurred from 500 to 700 μs after arc initiation (denoted by t = 0 in fig. 6). The theoretical value of the driver pressure p_4 for 100-percent efficiency, as obtained from equation (1), is indicated by a dashed line. The accelerometer output signal was used to infer the start of the diaphragm rupture. Interpretation of the accelerometer signals was speculative and thus the opening times denoted in figure 8 must be viewed as rough estimates. As mentioned previously, the steel diaphragms used in these tests rupture statically at an applied pressure of about 24 MPa, and the calculated opening time for

this diaphragm and applied pressure (ref. 11) is about 450 to 500 μs. Now, very high peak pressures were recorded early before apparent diaphragm rupture. Oscilloscope records indicated that disturbances on the pressure transducer output due to the arc discharge have subsided before the transducer experiences the initial driver-gas pressure increase shown in figure 8. Similar unreported measurements in the driver section of the arc-driven Langley 6-inch shock tube (ref. 8), in which the pressure port was blocked to isolate the pressure transducer from the driver pressure, demonstrated that acceleration effects on the transducer output were not significant. Hence, the data in figure 8 are believed to be a good indication of the local-pressure time history. These peaks indicate the existence of a system of shocks from the electric-arc discharge, implying nonuniform heating of the helium driver, and the reflection of these shocks from the diaphragm. As the diaphragm opens, the pressure drops rapidly as a result of the expansion wave propagating into the driver gas. The rise in pressure at later times indicates the passage of the shock (emanating from the arc discharge) that is reflected from the upstream surface of the rail assembly. Examination of the rail surfaces after the 5-MJ run indicated the arc had traveled approximately 1.0 m down the rail from its initial location during the time of arc discharge. Again, this travel implies the helium driver gas was not heated uniformly along the 2.44-m length.

The efficiency of energy conversion in the driver was determined from the incident shock velocity measured in the intermediate section of the expansion tube or in the driven section in the shock-tube mode of operation, as discussed previously. Typical variation of this velocity with axial distance downstream of the primary diaphragm is shown in figure 9 for air as the test gas. The values of incident shock velocity with distance were obtained from microwave traces, and the maximum value was used to determine the corresponding value of p_4 from simple shock-tube theory (ref. 11), and hence the efficiency. These values of efficiency are shown in figure 10 as a function of initial energy E for air and CO_2 as test gases. Roughly, the efficiency varies from 65 to 85 percent for air and from 30 to 60 percent for CO_2. The magnitude of these efficiencies is typical of those obtained in other electric-arc-driven facilities (for example, see refs. 5 and 8). In general, the efficiency tends to decrease with increasing energy. Such a trend has been observed in other studies. However, as a result of the variation in the number of capacitors, the test gas, and the initial test-gas pressure for the data of figure 10, no definite conclusions can be drawn concerning the variation of efficiency with energy.

The variation of the measured incident shock velocity in the intermediate section of the expansion tube at various energy levels is presented in figure 11. The velocities were determined from microwave records for air as the test gas and from time-of-arrival records for CO_2 as the test gas. Both the maximum values for air as the test gas and the values at the secondary diaphragm station ($x = 4.67$ m) for air and CO_2 as test gases are shown. As a result of the small number of instrumented stations in the intermediate section, the maximum value of the incident shock velocity for CO_2 as the test gas could not be inferred from time-of-arrival data. For air as the test gas at the lowest energy levels, the maximum value of the shock velocity in the intermediate section occurs at the diaphragm location. At the higher energy levels, corresponding to the higher values of incident shock velocity, the maximum value of the shock velocity occurs at a location ahead of the diaphragm. This trend contrasts with the results of

several shock-tube investigations which indicate that when shock strength is increased, the location of the maximum value of shock velocity in the driven section moves downstream (ref. 11). At the highest energy level, the attenuation from the maximum value to the value at the diaphragm station is about 10 percent.

Samples of the variation of incident shock velocity in the acceleration gas with distance along the acceleration section are shown in figure 12. These data were obtained with the microwave technique. For the lowest energy levels, a 5- to 10-percent attenuation in the velocity along the length of the section was observed for air and CO_2 as test gases. This magnitude of attenuation in velocity is approximately the same value reported in reference 1 for the same facility but with unheated helium driver gas. The velocity attenuation increased with increasing energy level and was about 15 percent for the highest energy level (E = 5 MJ).

The velocity of the incident shock wave at the exit of the acceleration section was significantly increased in the present tests as compared with the unheated helium driver tests of reference 1 in the same facility and for similar values of initial acceleration-section pressure. For example, the shock velocity at the end of the acceleration section for air as the test gas was approximately 4.8 km/s with unheated helium driver gas at a pressure of 34.5 MPa, compared with approximately 7.0 km/s for the highest energy level of the present tests.

Representative time histories of the measured wall static pressure in the driven and acceleration sections and the pitot pressure at the exit of the acceleration section are presented in figure 13. The wall pressure in the driven section (fig. 13(a)) decreases with time until the arrival of the reflected shock observed in the driver-gas pressure records. This shock arrives from 1 to 1.5 ms after the incident shock. Near the exit of the acceleration section, the time history of the wall pressure for the lowest energy level (fig. 13(b)) is similar to that reported in reference 1 for the unheated helium-driver mode of operation. However, at the higher energy levels, the acceleration-section wall pressure decreases rapidly after the arrival of the incident shock in the acceleration gas. This decrease in acceleration-section wall pressure is believed to be a result of both the nature of the flow and the inadequate thermal insulation of the sensing surface of the flush-mounted pressure transducer. (The negative deflection in fig. 13(b) for an energy of 3.47 MJ indicates the pressure transducer was not adequately insulated from thermal effects (ref. 1).) This hypothesis that the decrease in wall pressure is due to the nature of the flow is based on the fact that pressure transducers located in the acceleration section upstream of x = 19.7 m also demonstrated a rapid decrease in pressure after incident shock arrival, and the photomultiplier traces in figure 13(b) indicate a drop in signal concurrent with the drop in pressure.

Pitot pressures at the acceleration-section exit are shown in figure 13(c). Only two tests were made in which pitot pressure was measured, because of a number of hardware problems which were encountered with the electric drive system. These problems were of such a nature that a test model located at the acceleration-section exit would have been damaged extensively. Thus a degree of confidence in the hardware had to be established before installing a test model such as a pitot-pressure probe. These pitot pressures at the acceleration-section exit (test section) indicated very little, if any, quasi-steady test time for air as the test

gas. However, the results of reference 1 indicate time histories of acceleration-section wall pressure and pitot pressure are very sensitive to the initial value of the acceleration-gas pressure, which was not varied in the tests reported herein. Therefore, the optimum values of initial test-gas pressure and initial acceleration-gas pressure for expansion-tube operation were not obtained for the higher flow velocities generated with the arc-heated mode of operation, as compared with those reported in reference 1.

Some of the problems usually associated with electric drive systems were encountered, and these will now be discussed briefly. The surfaces of the insulators exposed to the hottest part of the arc deteriorated and had to be coated with room-temperature-vulcanizing rubber or were changed to a fluorogreen material. Carbon soot created by the extreme temperatures in the driver section permeated the entire interior of the facility during each run and required thorough cleaning of the facility. The electric-arc assembly had to be withdrawn after each run and thoroughly cleaned in order to pass an electrical breakdown test, although complete disassembly was not necessary. High-pressure seals confined the hot gases and soot to the immediate vicinity of the rail assembly prior to diaphragm rupture. One instance of arc-over occurred between the driver wall (at the ground potential) and the steel bolts securing the high-potential rail to the liner. Damage to the liner was extensive, but damage to the driver-vessel wall and the rail was slight. This problem was solved by replacing the steel bolts with nylon bolts. In some of the first tests with this arc-heated mode of operation, diaphragm tabs were sheared off and swept downstream. The installation of 3.2-mm-thick brass damper pads and the use of thicker diaphragms solved this problem. Occasionally, one of the capacitors in the energy storage system failed during discharge. Proper fusing prevented other capacitors in the bank from discharging into the failed capacitor and causing extensive damage. Mylar shields were also installed on the individual rows of capacitors to increase the creep path of the breakdown voltage and prevent individual shorts.

CONCLUDING REMARKS

The primary objective of this study was to evaluate the performance of a parallel-rail electric-arc system for generating high-density test-gas flow at the entrance of the nozzle of the expansion tunnel. A description was given of this parallel-rail electric-arc system for heating the helium driver gas in the Langley 6-inch expansion tube and the Langley expansion tunnel. The electrical characteristics and the efficiency of the system were inferred from measurements, and limited data were obtained to examine the performance of the expansion tube with the arc drive and with air and carbon dioxide as test gases.

The maximum value of peak current obtained was 2.5 MA with an initial stored energy of 5 MJ. The efficiency of conversion of electrical energy to thermal energy of the helium driver, as inferred from shock velocity measurements, was approximately 65 to 85 percent with one capacitor bank (2.5 MJ) and 30 to 60 percent when two banks were used. These efficiencies were inferred from simple shock-tube theory for thermochemical-equilibrium air and carbon dioxide as test gases, with measured incident shock velocity as an input. Measured pressures in the driver section just upstream of the diaphragm indicated the existence of a series of strong shocks generated in the helium driver as a result of the arc

discharge, rather than a steady rise in pressure with time. For this reason, measured driver pressures were not used to determine energy conversion efficiencies. This system of shocks in the driver section along with the observation that the arc did not travel the full length of the parallel rails, even at the highest energy level, implies the helium driver gas was not heated uniformly.

Measured values of the incident shock velocity in the intermediate section for air as a test gas indicate an initial acceleration of the shock, followed by a deceleration. The location at which the peak value of shock velocity occurred moved upstream with increasing shock velocity; this differs from the trend observed with an unheated helium driver gas in this same facility, as well as from the observations of a number of other shock-tube studies. The incident shock velocity in the acceleration section attenuated along the length of the section, and this attenuation increased with increasing energy level. At the highest energy, the attenuation was approximately 15 percent along the 17-m-long acceleration section.

Because of hardware problems encountered with the parallel-rail arrangement, only limited data were measured near the acceleration-section exit. The parallel-rail arc mode of operation increased the performance of the facility significantly in terms of free-stream velocity; however, wall static-pressure measurements near the exit of the acceleration section and pitot pressure at the test section indicated very little, if any, quasi-steady test time. Only a single value of the initial acceleration pressure was used for tests in which the pitot pressure was measured. Since test times are very sensitive to the initial acceleration-gas pressure, the optimum flow conditions for the parallel-rail mode of operation were not obtained in this study.

Langley Research Center
National Aeronautics and Space Administration
Hampton, VA 23665
October 29, 1976

REFERENCES

1. Miller, Charles G.: Operational Experience in the Langley Expansion Tube With Various Test Gases and Preliminary Results in the Expansion Tunnel. Paper presented at the AIAA Ninth Aerodynamic Testing Conference (Arlington, Texas), June 7-9, 1976.

2. Trimpi, Robert L.: A Preliminary Theoretical Study of the Expansion Tube, A New Device for Producing High-Enthalpy Short-Duration Hypersonic Gas Flows. NASA TR R-133, 1962.

3. Trimpi, Robert L.; and Callis, Linwood B.: A Perfect-Gas Analysis of the Expansion Tunnel, A Modification to the Expansion Tube. NASA TR R-223, 1965.

4. Friesen, Wilfred J.; and Moore, John A.: Pilot Model Expansion Tunnel Test Flow Properties Obtained From Velocity, Pressure, and Probe Measurements. NASA TN D-7310, 1973.

5. Dannenberg, Robert E.; and Silva, Anthony F.: Exploding Wire Initiation and Electrical Operation of a 40-kV System for Arc-Heated Drivers up to 10 Feet Long. NASA TN D-5126, 1969.

6. Moore, John A.: Description and Initial Operating Performance of the Langley 6-Inch Expansion Tube Using Heated Helium Driver Gas. NASA TM X-3240, 1975.

7. Jones, Jim J.; and Moore, John A.: Exploratory Study of Performance of the Langley Pilot Model Expansion Tube With a Hydrogen Driver. NASA TN D-3421, 1966.

8. Nealy, John E.: Performance and Operating Characteristics of the Arc-Driven Langley 6-Inch Shock Tube. NASA TN D-6922, 1972.

9. Panofsky, Wolfgang K.; and Phillips, Melba: Classical Electricity and Magnetism. Second ed. Addison-Wesley Pub. Co., Inc., c.1962.

10. Laney, Charles C., Jr.: Microwave Interferometry Technique for Obtaining Gas Interface Velocity Measurements in an Expansion Tube Facility. NASA TM X-72625, 1974.

11. Miller, Charles G., III; and Jones, Jim J.: Incident Shock-Wave Characteristics in Air, Argon, Carbon Dioxide, and Helium in a Shock Tube With Unheated Helium Driver. NASA TN D-8099, 1975.

12. Reller, John O., Jr.; and Reddy, N. M.: Analysis of the Flow in a 1-MJ Electric-Arc Shock Tunnel. NASA TN D-6865, 1972.

13. Miller, Charles G., III; and Wilder, Sue E.: Program and Charts for Determining Shock Tube, Expansion Tube, and Expansion Tunnel Flow Quantities for Real Air. NASA TN D-7752, 1975.

14. Miller, Charles G., III; and Wilder, Sue E.: Tables and Charts of Equilibrium Normal Shock and Shock Tube Solutions for Pure CO_2 With Velocities to 16 km/sec. NASA TM X-71982, 1974.

TABLE 1.- INITIAL CONDITIONS FOR EXPANSION-TUBE AND SHOCK-TUBE TESTS

Run no.	C, F	V, kV	E, MJ	Test gas	p_1, kPa	Acceleration gas	p_{10}, Pa
[a]69	0.0347	10	1.74	Air	6.89		
[a]70	.0347	10	1.74	Air	6.89		
67	.0347	11	2.10	Air	6.89	Helium	26.67
85	.0694	10	3.47	Air	6.89	Air	26.67
86	.0694	12	5.00	Air	6.89	Air	26.67
84	.0694	10	3.47	Air	48.26	Air	26.67
73	.0347	12	2.50	CO_2	24.13	CO_2	26.67
78	.0694	8.6	2.57	CO_2	24.13	CO_2	21.34
82	.0694	10	3.47	CO_2	48.26	CO_2	26.67
79	.0694	8.6	2.57	CO_2	24.13	CO_2	21.34

[a]Shock-tube runs.

TABLE 2.- CIRCUIT CONSTANTS DETERMINED FROM VOLTAGE AND CURRENT TIME HISTORIES

Run no.	C, F	V, kV	R, mΩ	L, μH	Frequency, rad/s	R/R_{cr}	n
[a]69	0.0347	10	3.17	0.60	7008	0.39	0.81
[a]70	.0347	10	4.16	.22	6634	.82	.86
67	.0347	11	3.72	.57	6283	.47	.83
73	.0347	12	3.11	.52	6798	.55	.67
78	.0694	8.6	2.44	.61	4437	.43	.36
82	.0694	10	2.57	.58	4469	.46	.32
84	.0694	10	2.15	.56	4680	.38	.36
85	.0694	10	2.09	.55	4734	.37	.62
86	.0694	12	2.29	.58	4904	.40	.62
79	.0694	8.6	3.64	.60	3854	.62	.36

[a]Shock-tube runs.

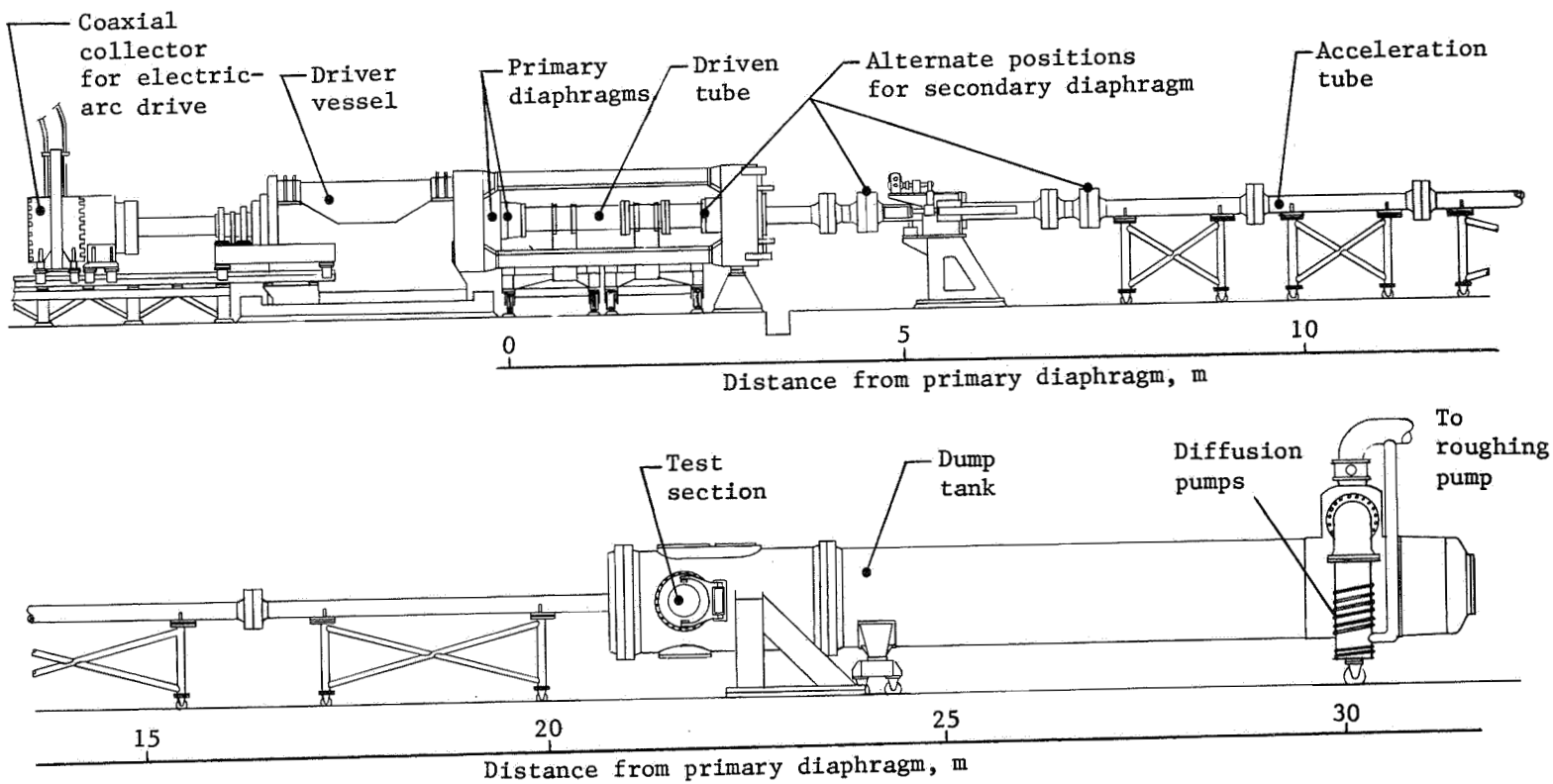

Figure 1.- Sketch of expansion tube.

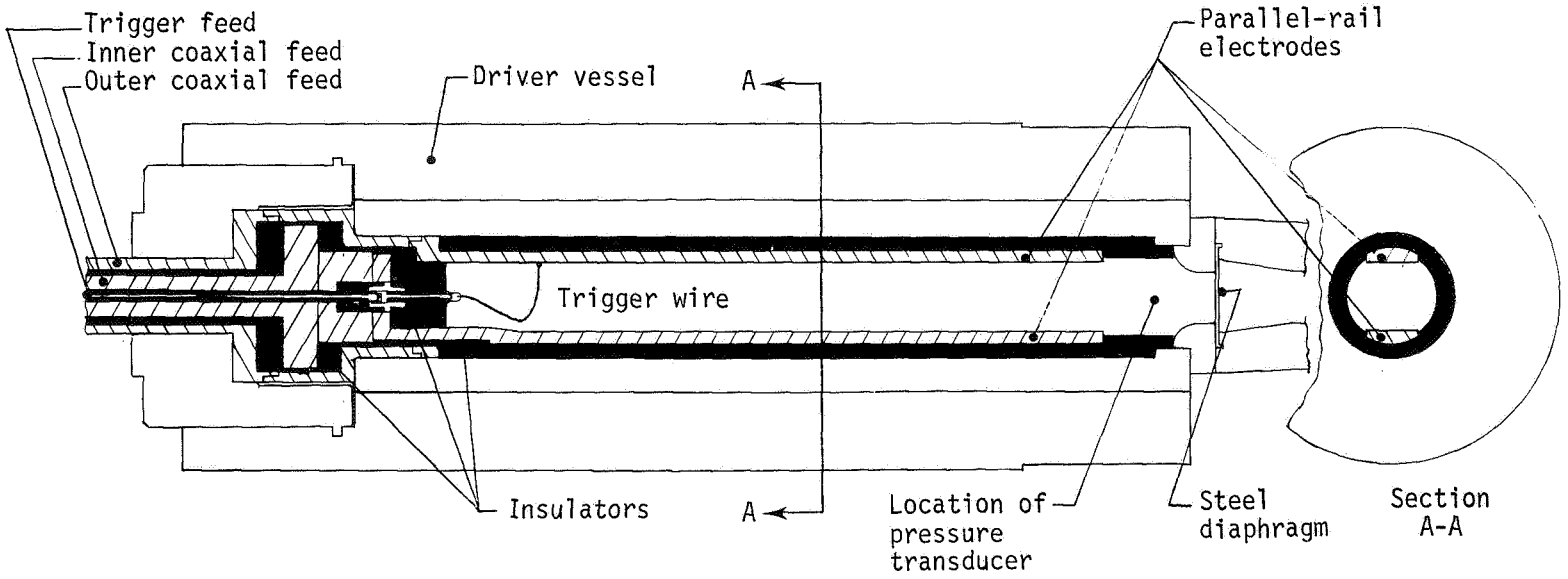

Figure 2.- Sketch of parallel-rail electric-arc driver configuration.

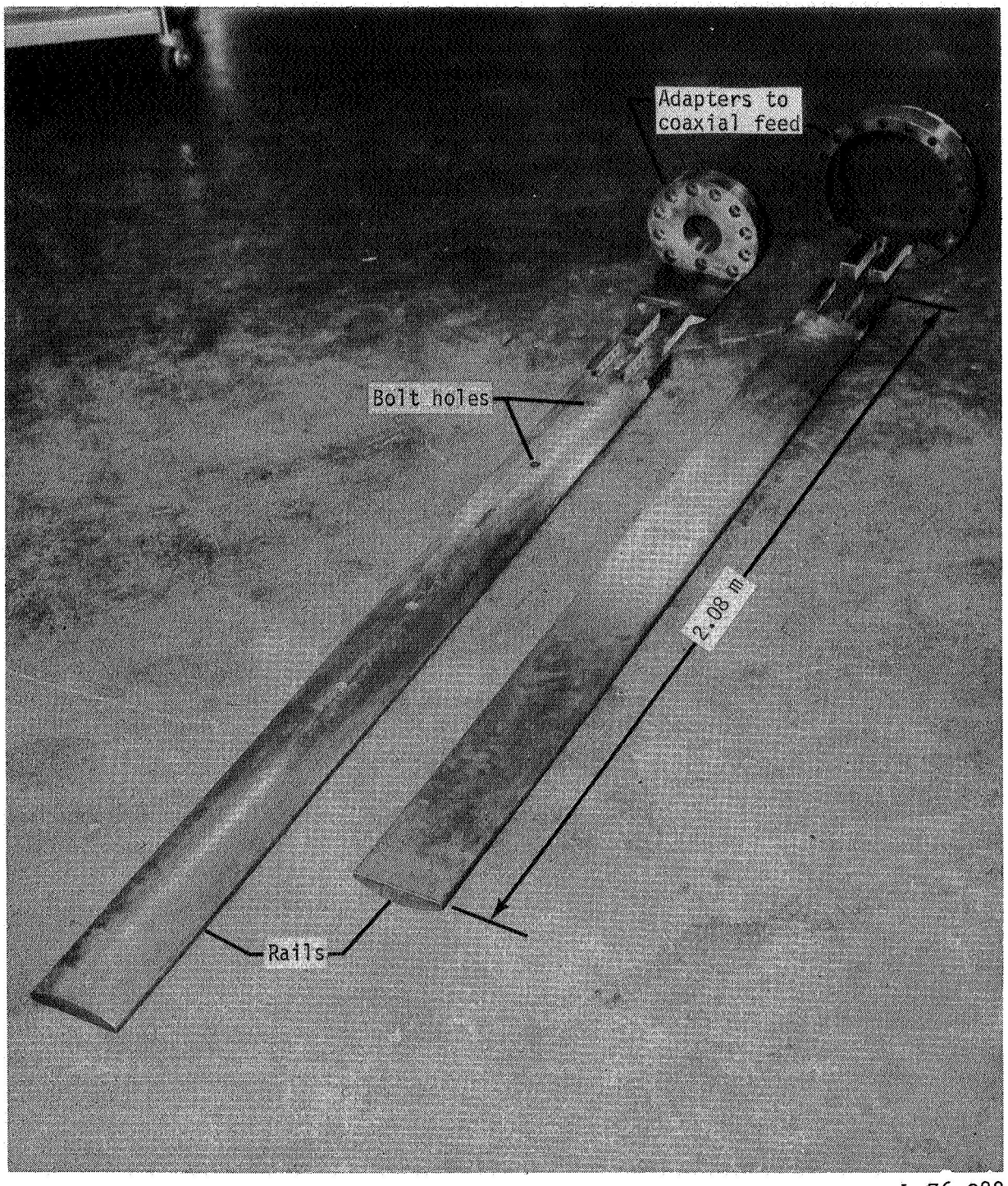

L-76-288

(a) Parallel rails, with adapters to coaxial electric feed.

Figure 3.- Photographs of basic components of electric-arc drive assembly.

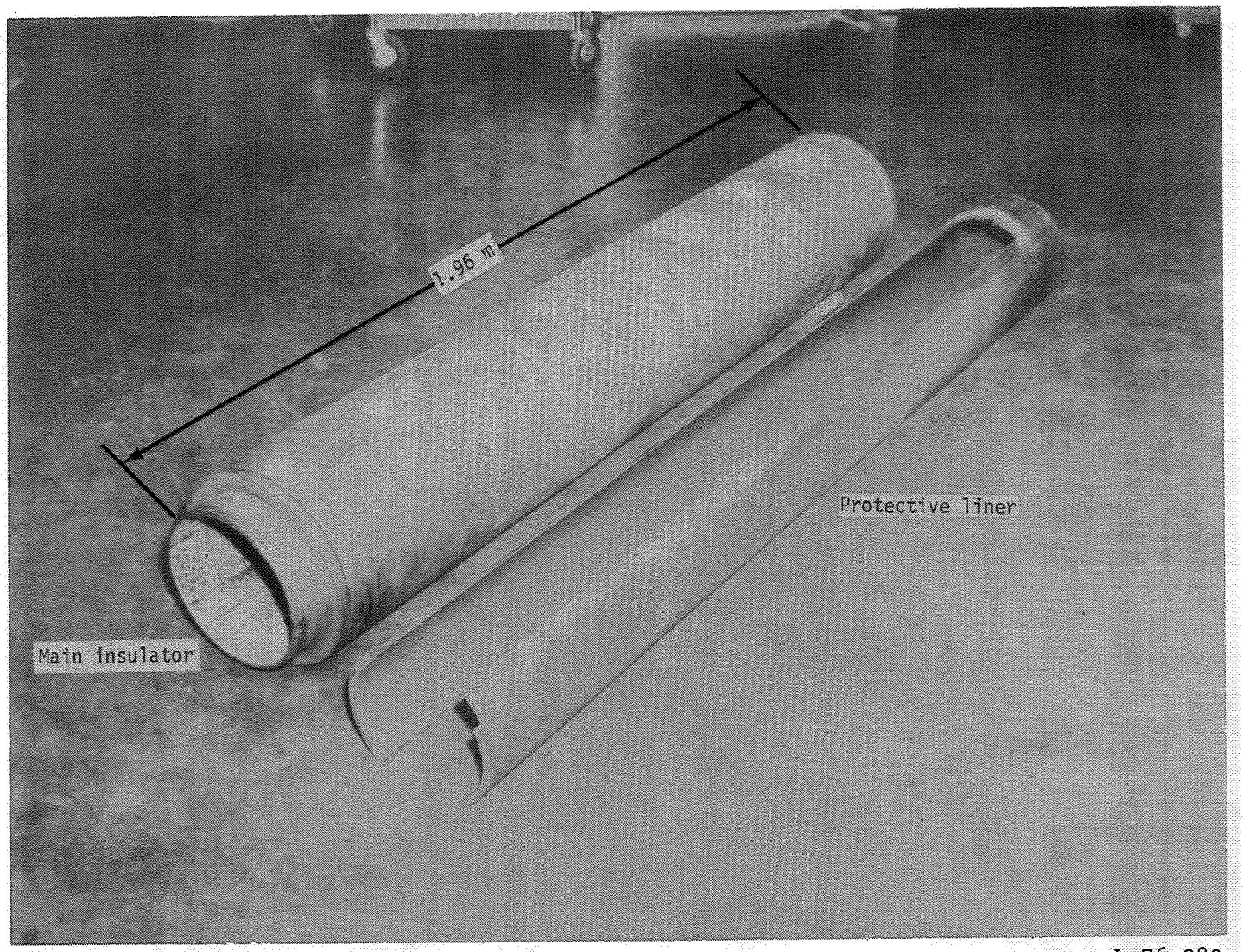

L-76-289

(b) Main insulator and protective liner.

Figure 3.- Continued.

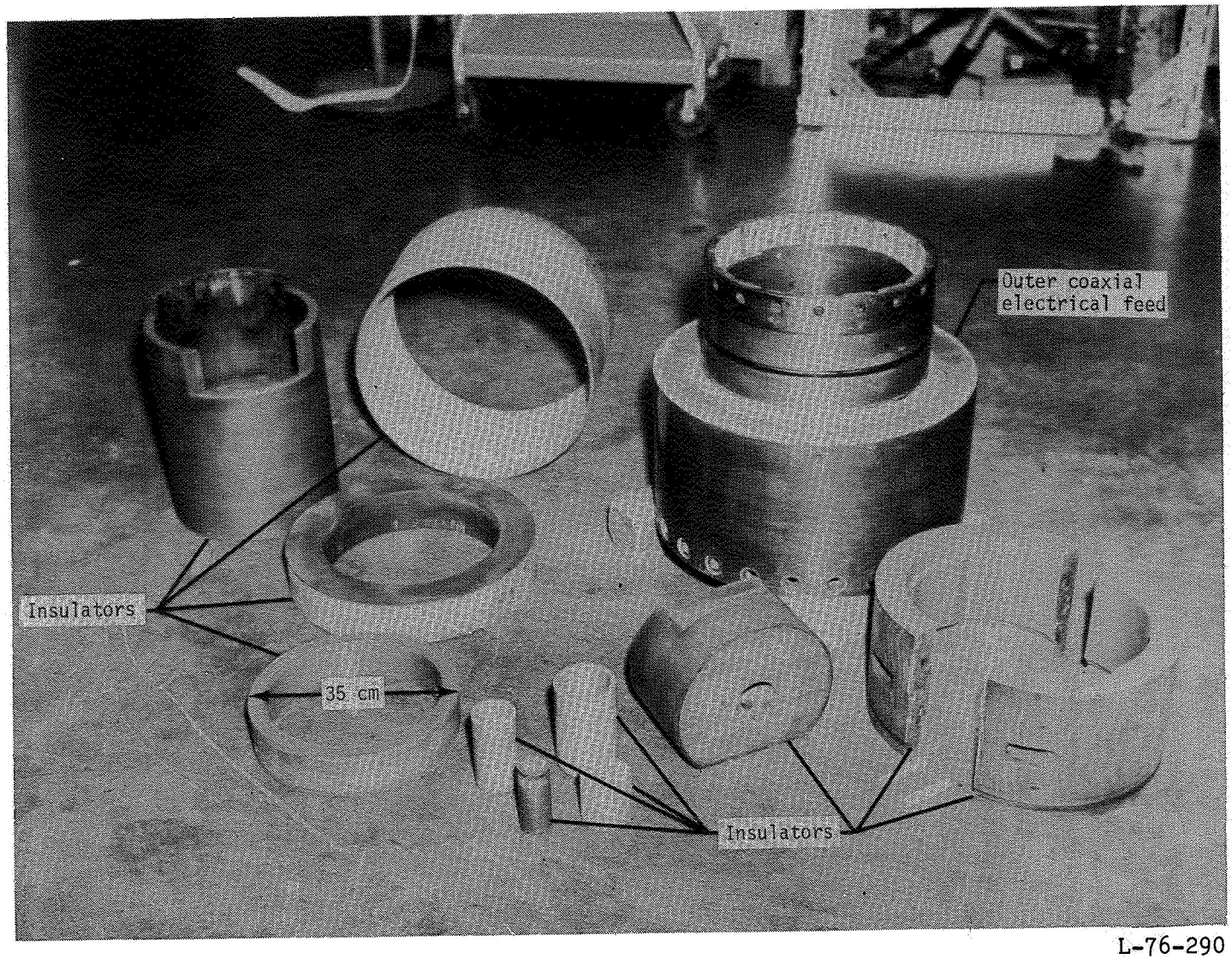

L-76-290

(c) Insulators and outer coaxial electrical feed.

Figure 3.- Continued.

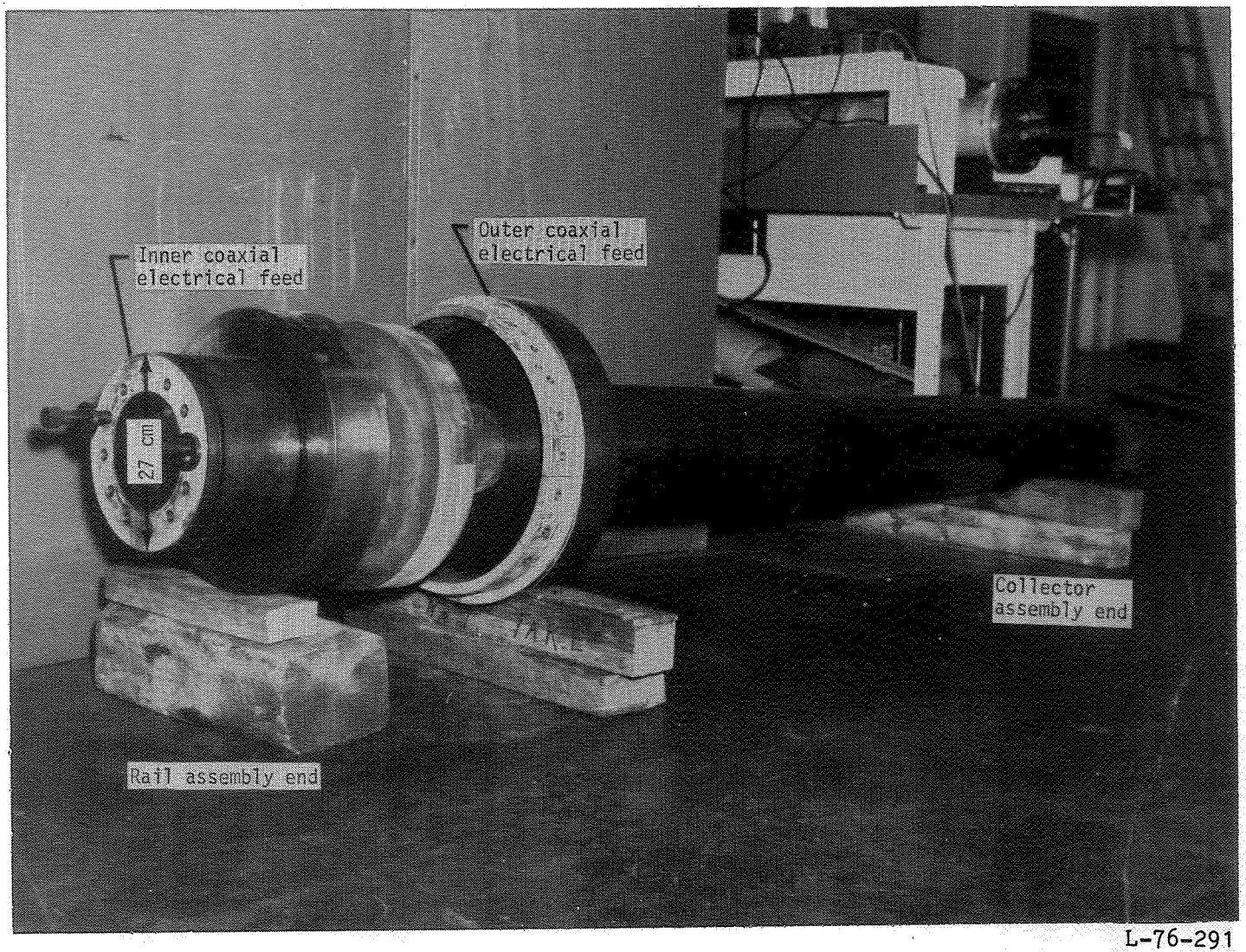

L-76-291

(d) Coaxial electrical feed from collector to rail assembly.

Figure 3.- Continued.

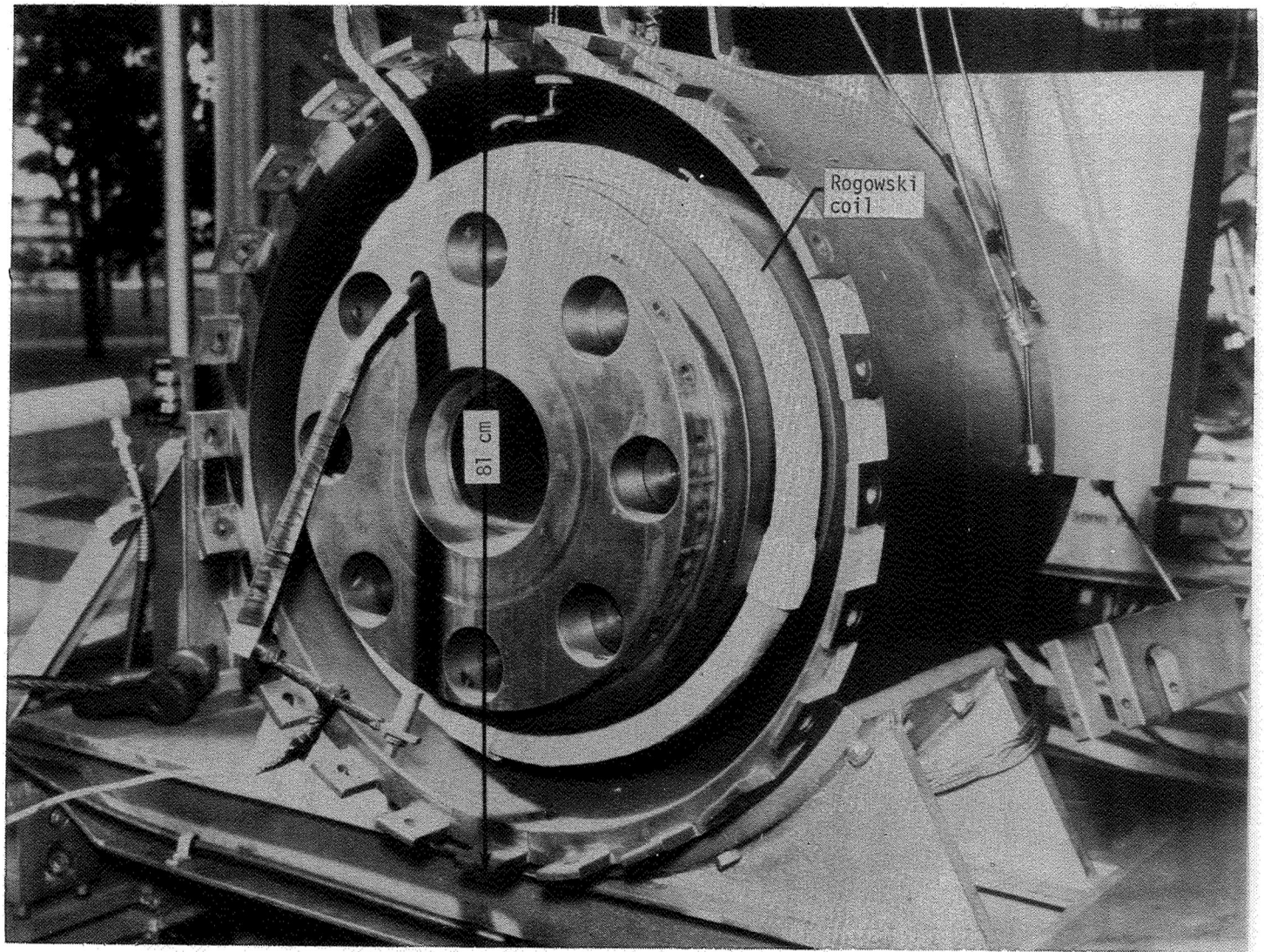

(e) Coaxial feed.

Figure 3.- Continued.

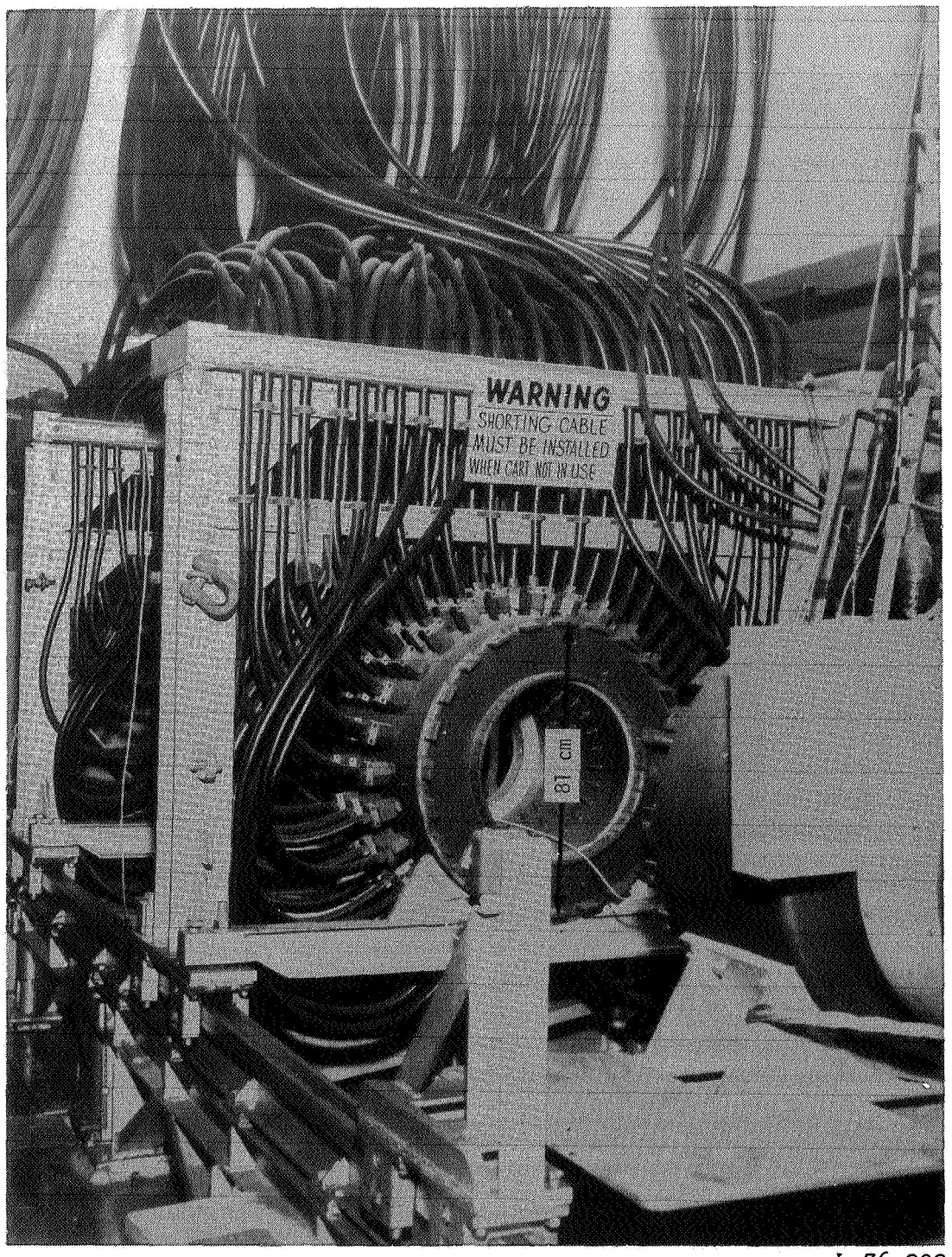

L-76-293

(f) Coaxial collector.

Figure 3.- Continued.

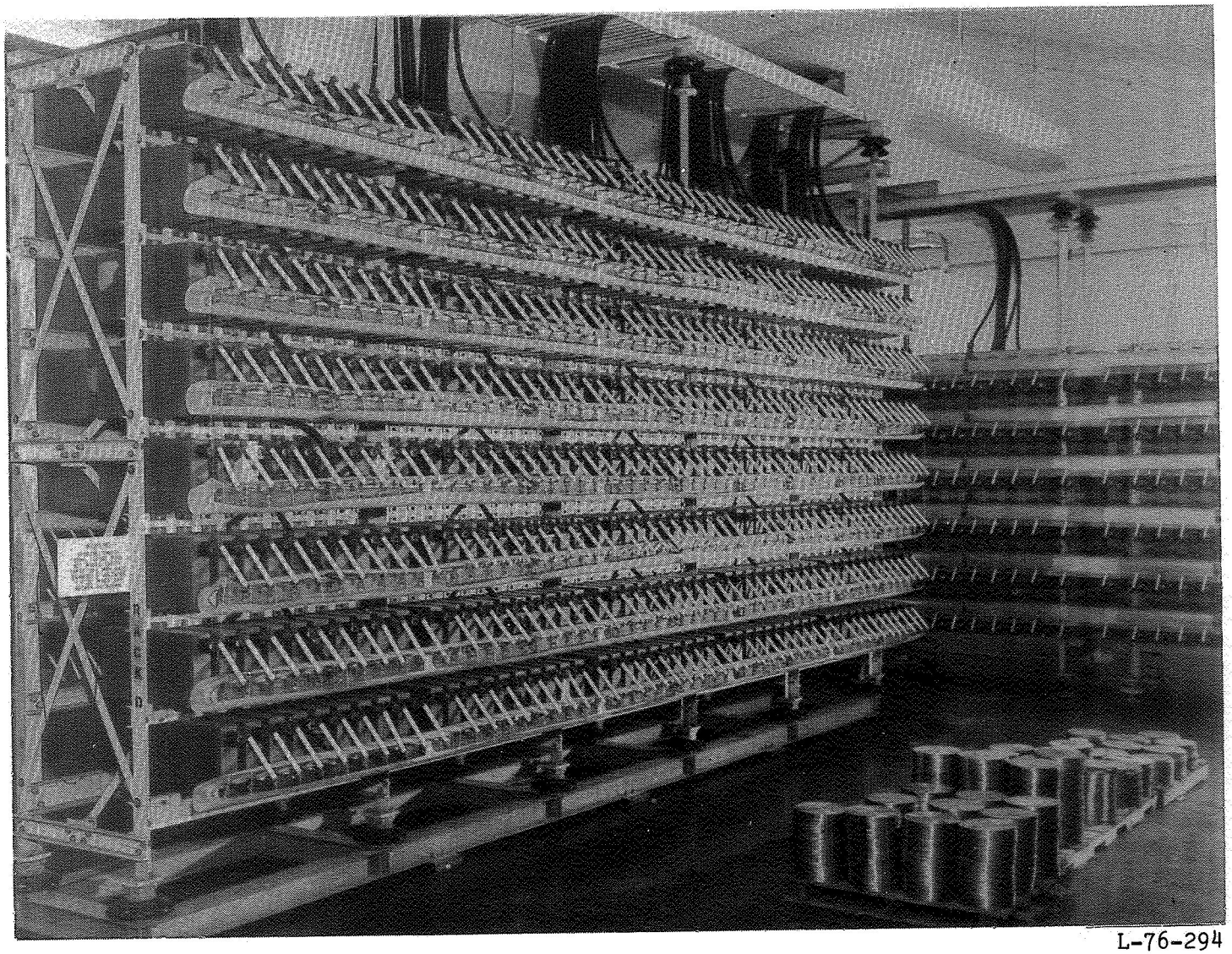

L-76-294

(g) Energy storage capacitor bank.

Figure 3.- Concluded.

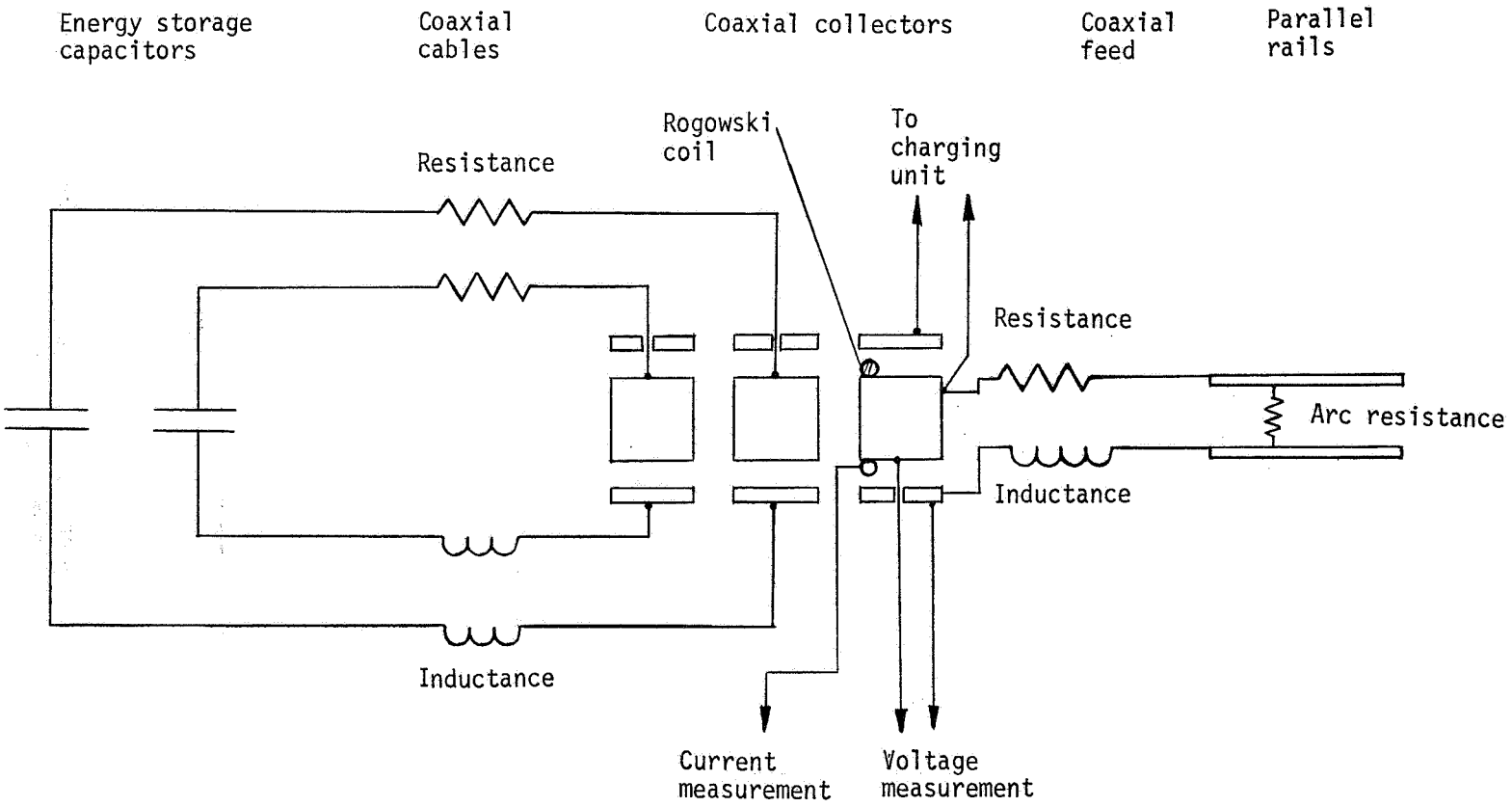

Figure 4.- Schematic of effective electrical circuit.

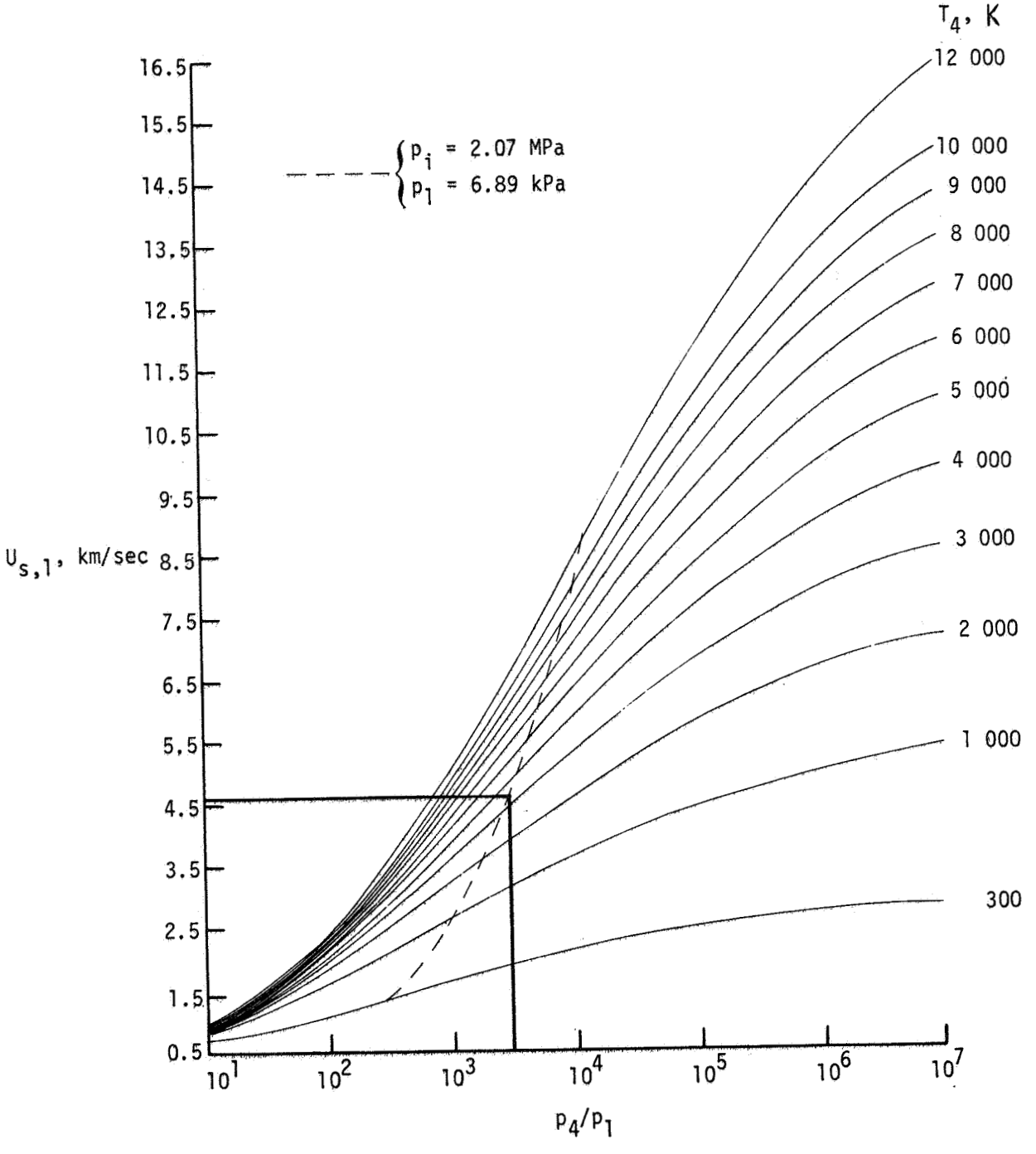

Figure 5.- Shock-tube performance for real-air test gas and helium driver gas over range of T_4.

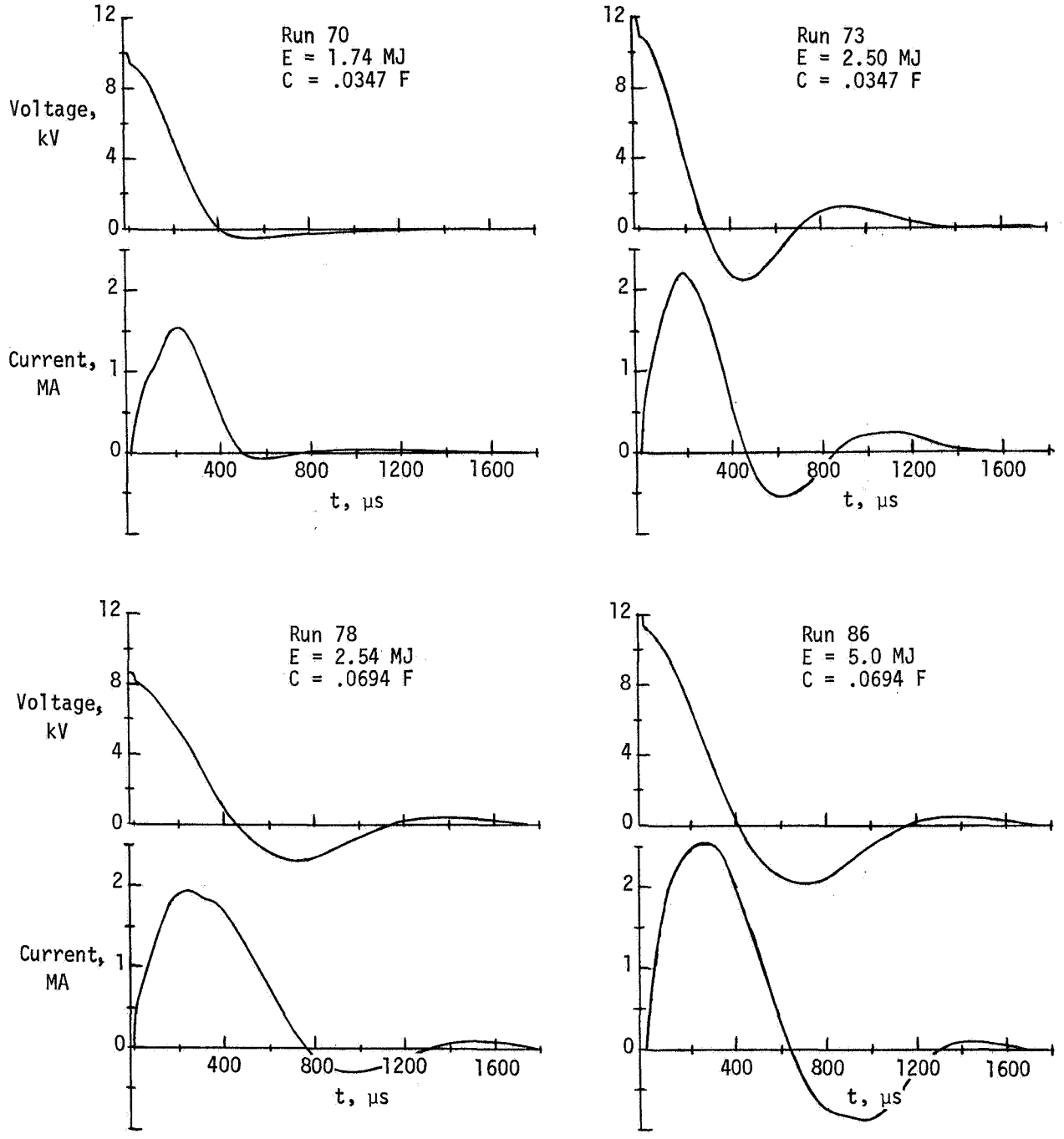

Figure 6.- Typical records of voltage and current during electrical discharge.

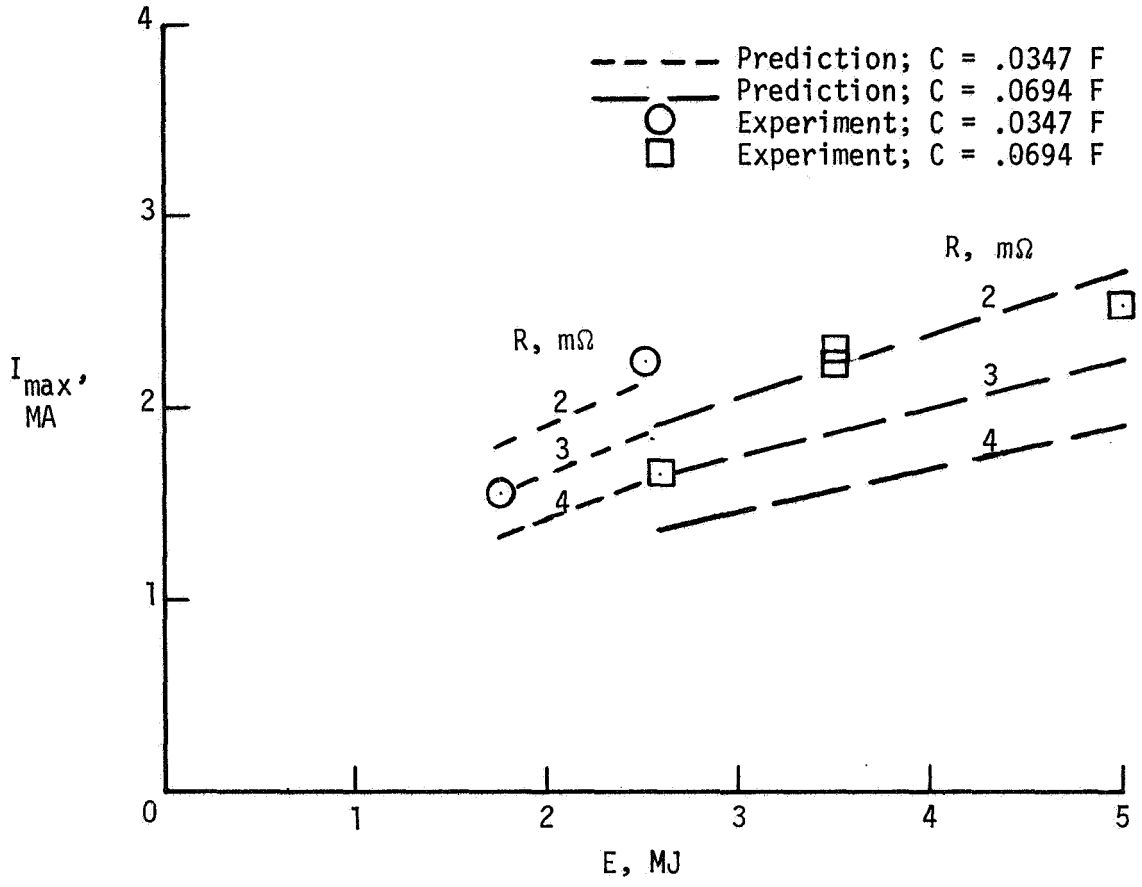

Figure 7.- Variation of maximum current with initial energy level.

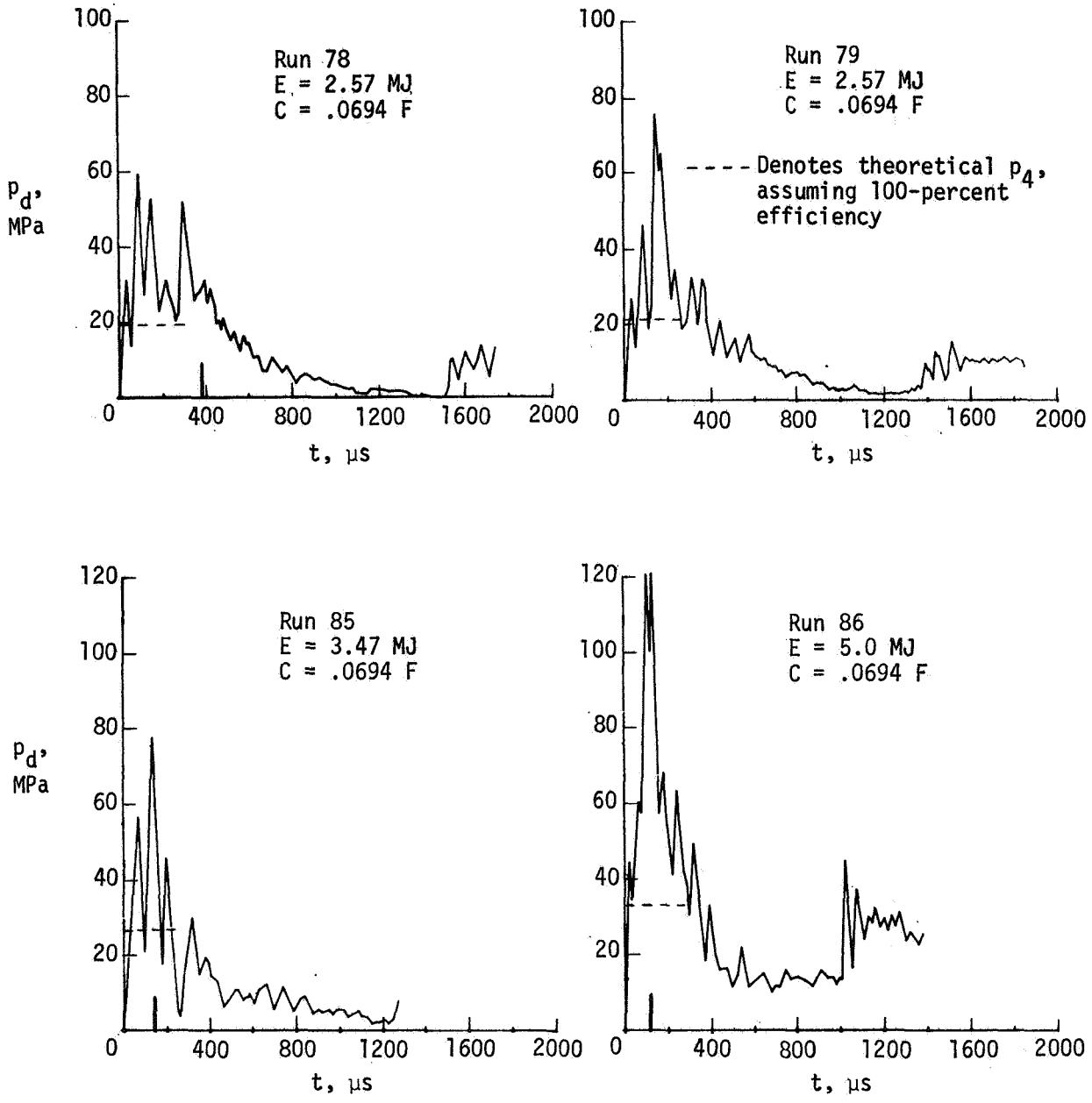

Figure 8.- Measured pressure in driver section as a function of time. Heavy tick mark denotes accelerometer indication of diaphragm opening.

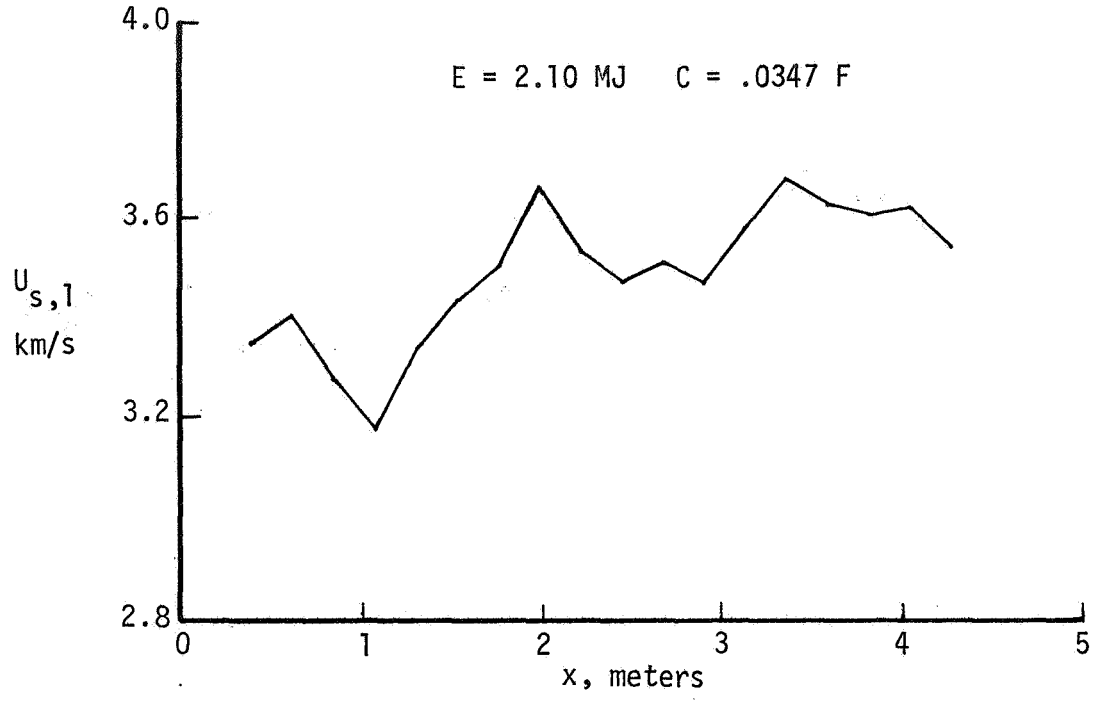

(a) Intermediate section of expansion tube.

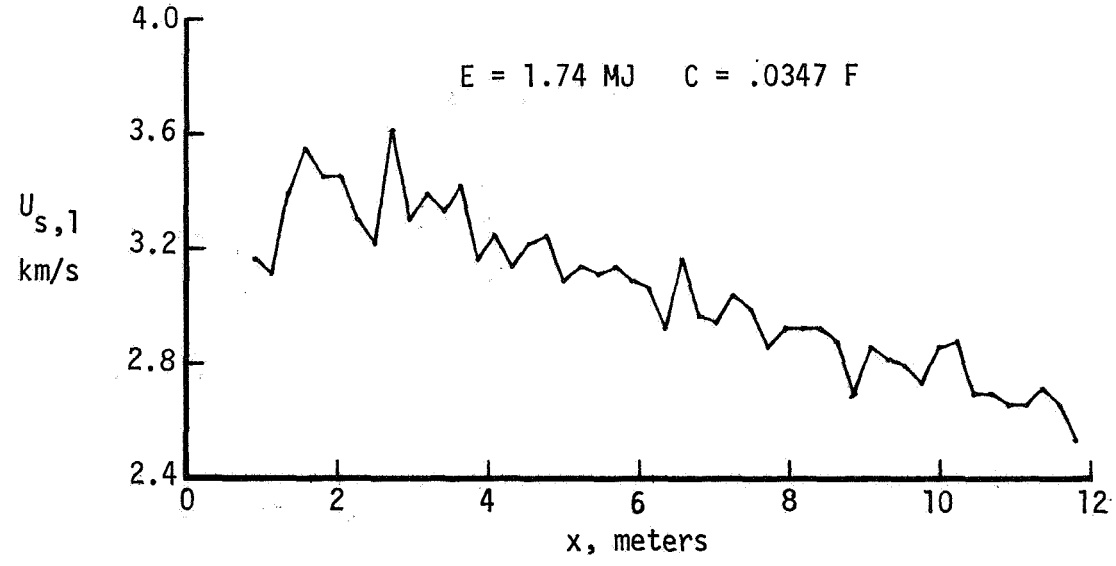

(b) Shock tube.

Figure 9.-Variation of incident shock velocity in air with axial distance downstream of primary diaphragm for expansion-tube and shock-tube modes of operation, using microwave technique.

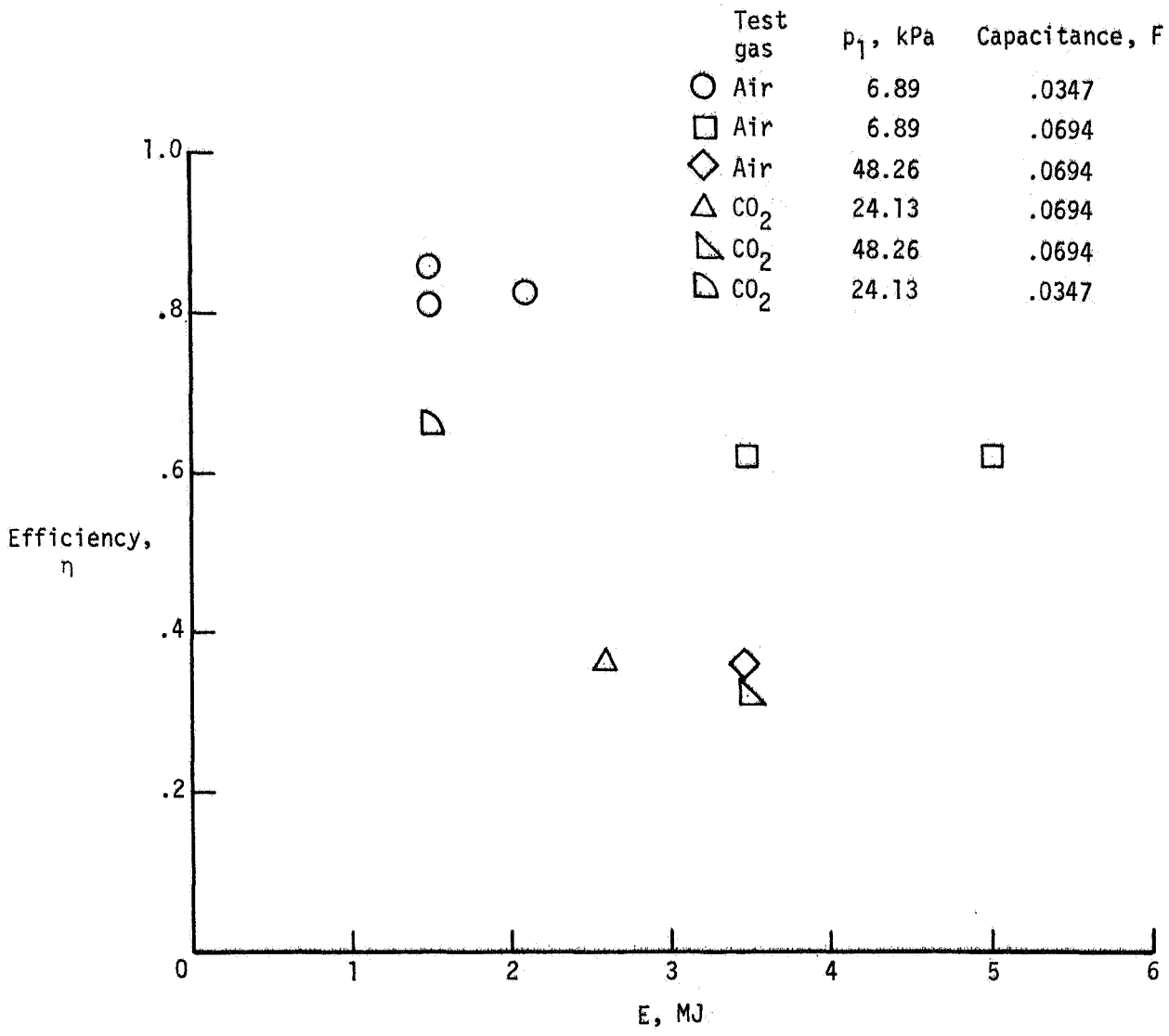

Figure 10.- Variation of efficiency of energy conversion in helium driver with initial energy level.

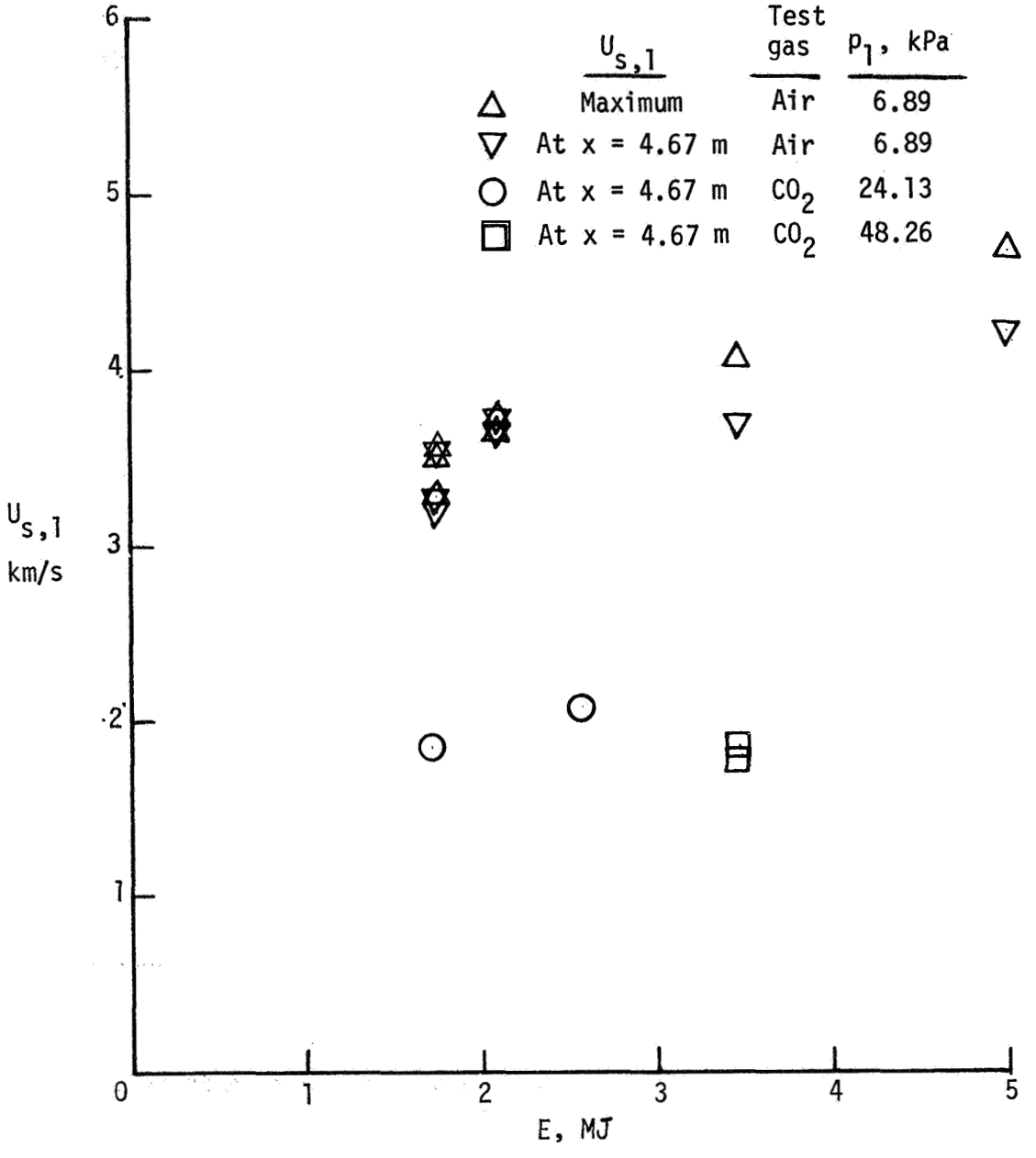

Figure 11.- Variation of shock velocity in intermediate section of expansion tube with initial energy level.

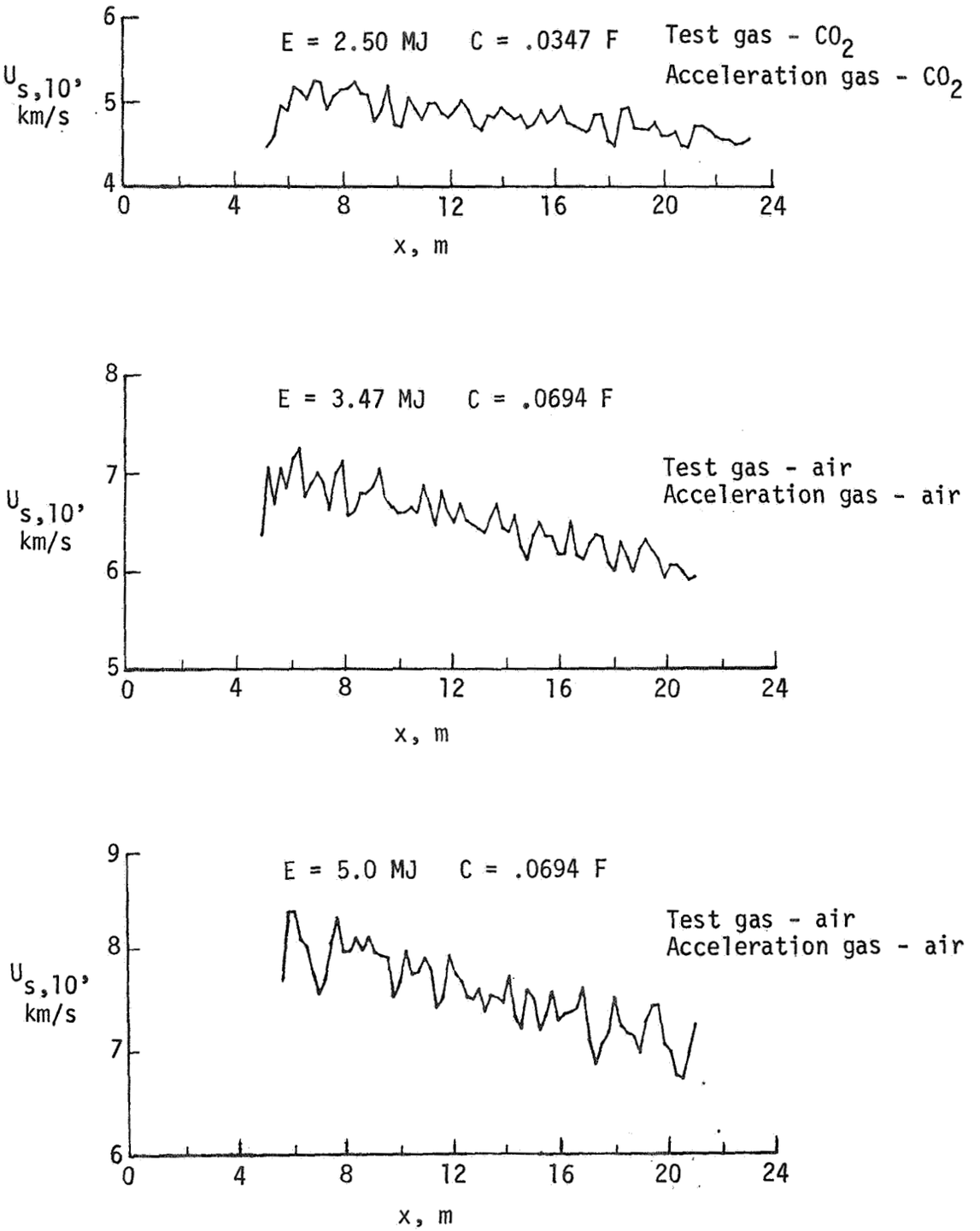

Figure 12.- Variation of incident shock velocity along acceleration section.

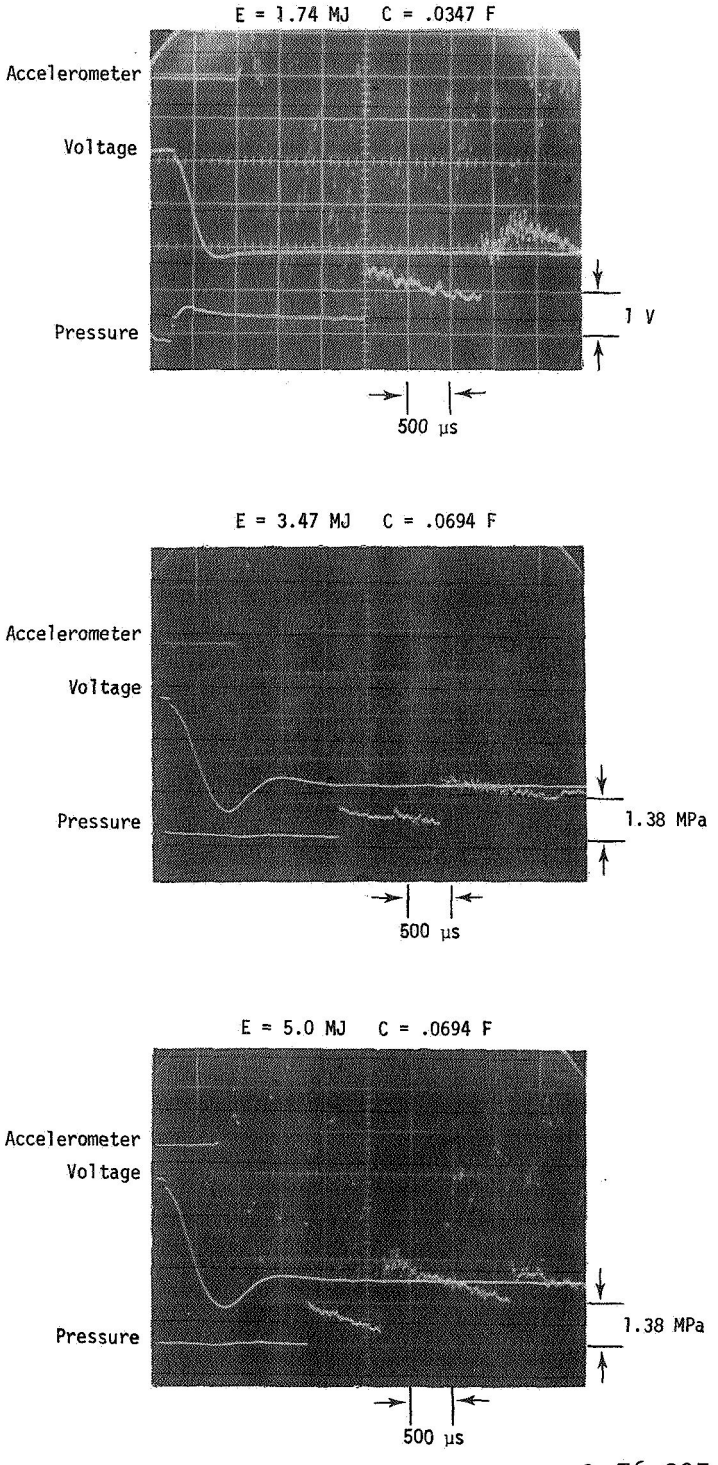

L-76-295

(a) Wall static pressure at x = 4.1 m (driven section). Accelerometer and voltage records also shown.

Figure 13.- Time histories of pressures in driven section and acceleration section of expansion tube. Air test gas at p_1 = 6.89 kPa.

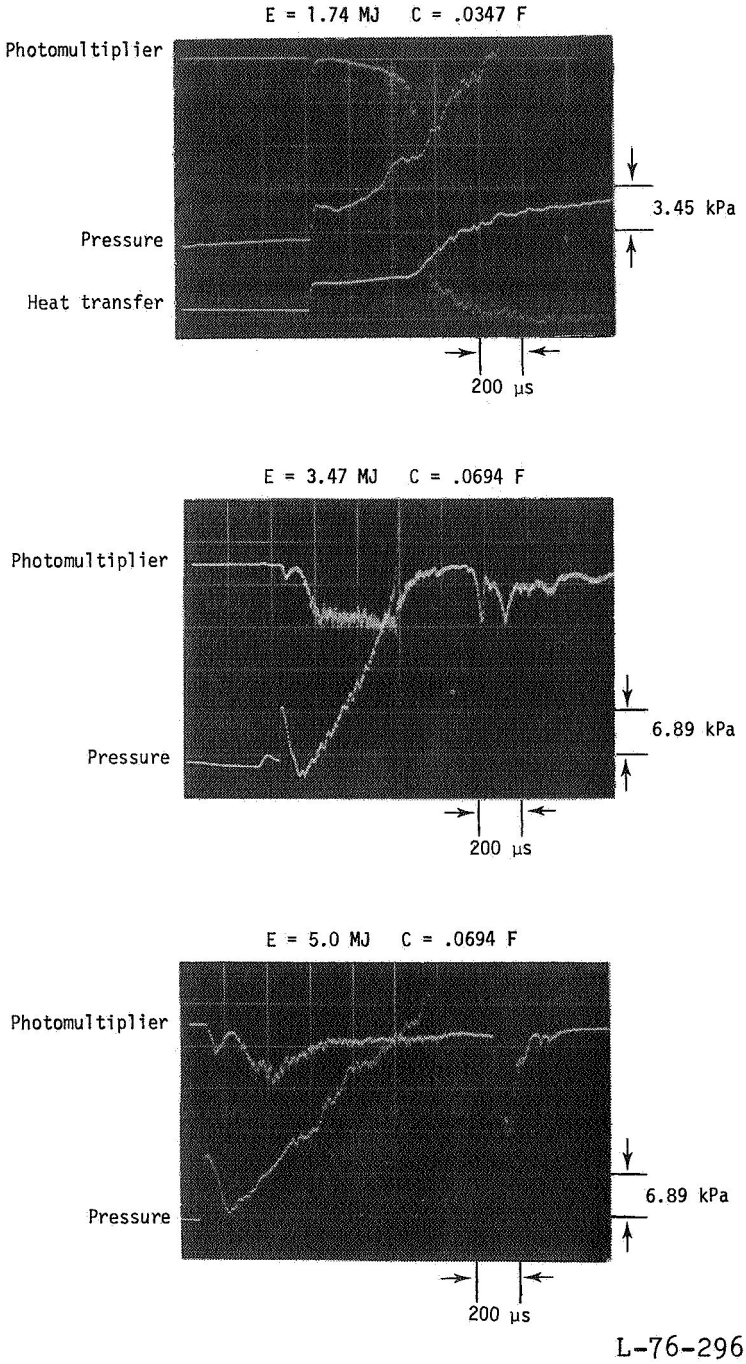

L-76-296

(b) Wall static pressure at x = 19.7 m (acceleration section). Photomultiplier and heat transfer records also shown.

Figure 13.- Continued.

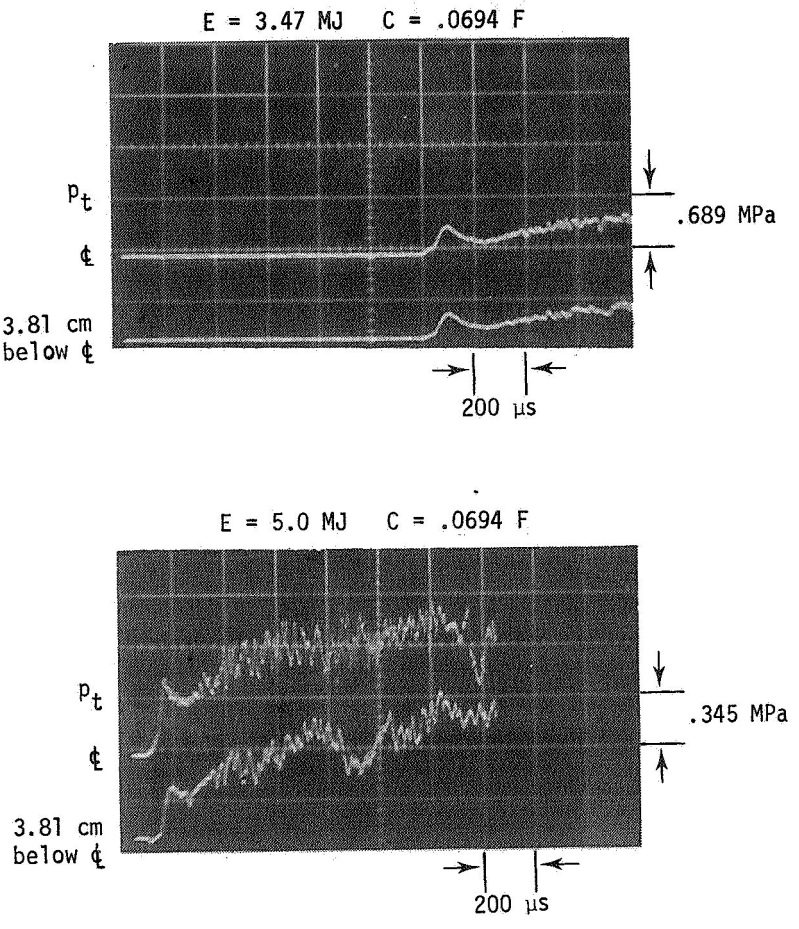

L-76-297

(c) Pitot pressure at acceleration-section exit.

Figure 13.- Concluded.

NATIONAL AERONAUTICS AND SPACE ADMINISTRATION
WASHINGTON, D.C. 20546

OFFICIAL BUSINESS
PENALTY FOR PRIVATE USE $300

SPECIAL FOURTH-CLASS RATE
BOOK

POSTAGE AND FEES PAID
NATIONAL AERONAUTICS AND
SPACE ADMINISTRATION
451

POSTMASTER: If Undeliverable (Section 158
Postal Manual) Do Not Return

"The aeronautical and space activities of the United States shall be conducted so as to contribute . . . to the expansion of human knowledge of phenomena in the atmosphere and space. The Administration shall provide for the widest practicable and appropriate dissemination of information concerning its activities and the results thereof."

—NATIONAL AERONAUTICS AND SPACE ACT OF 1958

NASA SCIENTIFIC AND TECHNICAL PUBLICATIONS

TECHNICAL REPORTS: Scientific and technical information considered important, complete, and a lasting contribution to existing knowledge.

TECHNICAL NOTES: Information less broad in scope but nevertheless of importance as a contribution to existing knowledge.

TECHNICAL MEMORANDUMS: Information receiving limited distribution because of preliminary data, security classification, or other reasons. Also includes conference proceedings with either limited or unlimited distribution.

CONTRACTOR REPORTS: Scientific and technical information generated under a NASA contract or grant and considered an important contribution to existing knowledge.

TECHNICAL TRANSLATIONS: Information published in a foreign language considered to merit NASA distribution in English.

SPECIAL PUBLICATIONS: Information derived from or of value to NASA activities. Publications include final reports of major projects, monographs, data compilations, handbooks, sourcebooks, and special bibliographies.

TECHNOLOGY UTILIZATION PUBLICATIONS: Information on technology used by NASA that may be of particular interest in commercial and other non-aerospace applications. Publications include Tech Briefs, Technology Utilization Reports and Technology Surveys.

Details on the availability of these publications may be obtained from:

SCIENTIFIC AND TECHNICAL INFORMATION OFFICE

NATIONAL AERONAUTICS AND SPACE ADMINISTRATION

Washington, D.C. 20546